# Cheating on orthogonal social traits prevents the tragedy of the commons in *Pseudomonas aeruginosa*

Özhan Özkaya, Roberto Balbontín, Isabel Gordo and Karina B. Xavier#

Instituto Gulbenkian de Ciência, Oeiras, Portugal

Running Head: Ecology of multiple social traits

#Address correspondence to Karina B. Xavier, kxavier@igc.gulbenkian.pt

## Abstract

Bacterial cooperation can be disrupted by non-producers, which can access public goods without paying their production cost. These cheaters can increase in frequency, exhausting the public goods and causing a population collapse. We investigated how interactions among cheaters in orthogonal social traits influence such collapse. We characterized the dynamics of Pseudomonas aeruginosa polymorphic populations under conditions where two social traits, production of iron-scavenging pyoverdine and quorum sensing regulated elastase, are necessary. We demonstrate that cheaters for either trait compete with both the wild type and each other and, since production of pyoverdine is costlier than elastase production, pyoverdine cheaters impair invasion by quorum sensing mutants, preventing the collapse caused by the latter. A mathematical model shows that these dynamics are determined by the costs of the social traits involved, while their benefits only influence population mean fitness. Finally, we show how quorum sensing regulation can avoid full loss of cooperation.

## Introduction

Although bacteria are unicellular organisms, they can engage in many group behaviors including biofilm formation, swarming motility, production and secretion of extracellular proteases and iron-chelating siderophores (1–4). The collective production of costly, secreted compounds provides fitness benefit to the entire population and can be considered as cooperative behaviors. Cooperation is frequently under the threat of exploitation by cheaters: individuals that benefit from the cooperative action but contribute little or nothing at all to the production of the public goods. When mixed with cooperators, cheaters can increase in frequency and cause loss of cooperation by exhaustion of the public goods, leading to a collapse of the entire population, characterized by a strong decrease in the growth yield of the entire population (5). This phenomenon, defined as the ‘tragedy of the commons’, was coined in economics (6), but has been explored in ecology (7) and has also become a focus of attention in microbiology in the last decade (8–12). Several mechanisms have been proposed to explain how cooperative behaviors are still

observed and maintained in microbial populations despite the emergence of cheaters. For instance, spatial structure and diffusion (13–22), pleiotropy (9, 23–30), migration (31), social and non-social adaptations (7, 11, 32, 33), policing mechanisms (10), molecular properties of public goods (34), and metabolic strategies (35) play significant roles in maintaining cooperation by preventing cheater invasions and avoiding the tragedy of the commons (2). Importantly, despite all these mechanisms to inhibit cheaters' invasion, cheating behavior is still observed *in vitro* (9–11, 25), *in vivo* (36, 37), and in natural populations (38–40).

Certain cheaters are also clinically relevant and are repeatedly isolated from the sputum samples of cystic fibrosis (CF) patients chronically infected with *Pseudomonas aeruginosa* (38, 41–43). CF is a genetic disorder which causes thickening of mucus in the lungs. Although initial acute infections are normally associated with colonization of the lungs by wild type (WT) *P. aeruginosa*, subsequent chronic infections consist of polymorphic populations which include mutants affected in social traits (41, 43–45). Importantly, *in vitro* studies, which focused on one trait and one constraint at a time, demonstrated that invasion by a cheater leads to a tragedy of the commons (9–11). However, despite the prevalence of social cheaters in the CF lung population, population collapse due to the invasion of cheaters has not been described. Therefore, we reasoned that studying interactions among multiple social cheaters, simultaneously, under conditions where more than one social trait is required could provide new insights into socialdynamics of *P. aeruginosa* populations in CF lungs and other environments. When more than one environmental constraint is present, the roles among different social mutants are likely to be more complex, since a cheater for one trait could potentially be a cooperator for another, making 'cheater' and 'cooperator' relative terms (46). We hypothesize that in environments where multiple constraints require bacteria to express multiple cooperative traits simultaneously, competition among mutants in orthogonal social traits (traits that are not known to be functionally linked), could influence their co-existence and the magnitude of the collapse of the population. This possibility is further supported by recent theoretical and experimental studies showing that interactions between interlinked cooperative traits significantly affect the course of their evolution (26, 47).

Here we examine the consequences of ecological interactions among social cheaters and the full cooperator in *P. aeruginosa* populations under conditions where two orthogonal cooperative traits are required.

Both *lasR* and *pvdS* mutants are used individually in a large number of sociomicrobiology studies (9, 25, 34, 48–52) and are among the most common mutants recurrently isolated from the sputum samples of CF patients (38, 41, 42). LasR is the master regulator of quorum sensing (QS) and controls the production of elastase. Production and extracellular secretion of elastase is essential for *P. aeruginosa* to digest complex sources of amino acids, such as casein, which serves as carbon and nitrogen source (9). Previous studies showed that *lasR* mutants grow poorly in media containing casein as the only carbon source, but increase in frequency when mixed with WT bacteria. This invasion of the mutant, eventually leads to a collapse where the total cell numbers of the population are drastically reduced due to the depletion of producers of the essential public good (9–11). Similarly, production of pyoverdine is one of the most studied cooperative trait in bacteria (34, 48–52). In iron-limited environments, pyoverdine is secreted by the *P. aeruginosa*, chelates iron from the environment and is subsequently retrieved, providing iron to the cell (49). Mutants in pyoverdine synthesis (e.g. *pvdS*) do not pay the cost of its production but are still able to retrieve the iron-bound pyoverdine produced by others, gaining a fitness advantage and increasing in frequency in the population (34, 53, 54).

We followed the cheating behavior of a *lasR* knock-out (KO) mutant in environments where casein is the sole carbon source, and thus production of elastase is required. In addition to this 'one constraint - one trait' setting, we added another constraint (iron depletion) and another social player (a *pvdS* KO mutant) and studied the behavior of the population in a 'two constraints - two traits' setting. We quantified the cheating behavior of a *lasR* mutant in short and long-term competitions, in iron-supplied or iron-depleted casein media with or without the presence of a *pvdS* mutant. We found that the relative fitness of the *lasR* mutant is altered when the *pvdS* mutant is in the culture, but only when the *lasR* mutant produces pyoverdine. We next determined the long-term consequences of the interactions among the two mutants and the WT for the onset of the tragedy of the commons. Our results show that in the environment

where the two cooperative traits are required, competition between the two mutants affects their dynamics, preventing the drastic population collapse otherwise caused by domination of the *lasR* mutant. Moreover, we developed a mathematical model which shows that social dynamics in multiple public good competitions are determined by the differences among the costs of the public goods involved, while their benefits only affect population mean fitness.

## Results

### *Cheating behavior of* lasR *mutant depends on the environment and the composition of the population.*

We investigated the fitness of *lasR* and *pvdS* mutants, alone and in competition under different environmental conditions, to determine the effect of the interactions between different cooperative traits on the dynamics of the cheater frequency and on the overall fitness of the population. Both mutants grow as well as WT in media where neither elastase nor pyoverdine are required (*i.e.*, an iron-supplied medium where casamino acids (CAA) are the sole carbon source) (Fig. S1*A*). However, when casein is the sole carbon source, *lasR* mutant has a lower growth than WT (Fig. S1*B*) and in iron-depleted CAA medium the growth yield of *pvdS* mutant is lower than that of WT and *lasR* mutant (Fig. S1*C*). Importantly, even though LasR regulates most of the quorum sensing genes in *P. aeruginosa*, the growth yield of *lasR* mutant was only affected significantly in media where elastase is required (Fig. 1 and Fig. S1). These data corroborate that there is no direct functional link between *lasR* and *pvdS* under the conditions tested (Fig. S1*B* and S1*C*) (55, 56). Next, to obtain a condition where both constraints were present, we cultured these mutants in a medium with casein as the sole carbon source supplemented with transferrin to deplete iron (iron-depleted casein medium). Monocultures of both *lasR* and *pvdS* mutants have a lower growth yield than WT in this medium (Fig. 1) because, under these conditions, elastase and pyoverdine are both required for growth. Importantly, the growth yield of *lasR* mutant is smaller than that of *pvdS* mutant.

We next determined the relative fitness of these two mutants in competition with WT. When there is no environmental constraint present, neither of the mutants show any significant increase in frequency (Fig. S2*A*). However, when co-cultured with WT in iron-supplied casein medium, *lasR* mutant increases in frequency, demonstrating that it can act as cheater under these conditions (Fig. 2*A*-left and Fig. S2*B*). Introduction of the *pvdS* mutant in the WT:*lasR* co-cultures does not affect the cheating behavior of *lasR* mutant, since *lasR* can also increase in frequency in the triple co-culture (Fig. 2*A*-right, and Fig. S3*A*). The fact that *pvdS* mutant does not change the behavior of *lasR* mutant in the iron-supplied casein media is consistent with the fact that *pvdS* mutant does not increase in frequency, and thus it does not act as a cheater under these conditions (Fig. 2*B* and Fig. S3*B*). Then, we studied the behavior of these mutants in the medium with two constraints (iron-depleted casein medium). In this medium, *lasR* mutant again increases in frequency in the co-cultures with WT (Fig. 2*C*-left). Importantly, the relative fitness of *lasR* in iron-depleted casein medium is smaller than the observed in the iron-supplied casein medium (Fig. 2*A*-left). This is not due to a differential production of pyoverdine in *lasR* (Fig. S4) but because, in iron-depleted casein medium, WT reaches a much smaller growth yield than in iron-supplied casein medium (Fig. 1 and Fig. S1*B*). In fact, when measured in units of cumulative numbers of cell divisions (CCD = final cell number – initial cell number) (57, 58) the relative fitness per cell division of *lasR* is not significantly different in the two media ($7.27 \times 10^{-10} \pm 2.19 \times 10^{-10}$ versus $7.53 \times 10^{-10} \pm 1.20 \times 10^{-10}$ in iron-supplied and iron-depleted medium, respectively) and thus the relative fitness of the mutants in 48 hours (Fig. 2) is higher in the iron-supplied medium, where the growth yield is also higher (Fig. 1).

Interestingly, when *pvdS* mutant added to the competition in iron-depleted casein medium, it acts as a cheater in co-cultures with WT (Fig. 2*D*-left), and in triple cultures with *lasR* and WT (Fig. 2*D*-right, and Fig. S3*D*). Strikingly, in the triple cultures under the condition where both traits are required, the presence of *pvdS* mutant results in a significant decrease in the ability of *lasR* mutant to act as a cheater (Fig. 2*C*-right, and Fig. S3*C*). These results show that the costs and benefits of the two social traits studied here are context dependent and support the conclusion that the behaviors of the social

mutants vary not only with the environment, but also with the level of polymorphism in the population.

### *Cheating capacity of* lasR *mutant determines the onset of the tragedy of the commons*

We next asked what would be the long-term consequences of these differences in cheating capacities for the overall fitness of the population by performing long-term propagations (Fig. 3). We started co-cultures with WT:*lasR* or WT:*lasR*:*pvdS* (at 9:1 and 8:1:1 initial ratios, respectively), in either iron-supplied casein medium (Fig. 3*A* and 3*B*), or in iron-depleted casein medium (Fig. 3*C* and 3*D*). The illustrations of the four experimental conditions are shown in Fig. S5. Propagations were performed by culture transfer to fresh media every 48 hours. Before each passage, cell density and frequencies of WT, *pvdS,* and *lasR* cells were determined. Growth yields in $OD_{600}$ and colony forming units (CFUs) are shown in Fig. 3 and Fig. S6, respectively.

We observed that, in the long-term propagations, in five out of six replicates of WT:*lasR* co-cultures in iron-supplied casein medium, *lasR* mutant quickly increased in frequency throughout the first 8 days (4 passages), reaching up to 90% of the population (red bars in Fig. 3*A*). The total cell densities of the populations (black lines) rapidly decreased to levels similar to that of *lasR* monocultures ($OD_{600}$ = 0.03) by day 12, and no recovery was observed in subsequent passages (Fig. 3*A*, and Fig. S7). We defined this density, which was reached by day 12 of the propagation ($OD_{600}$ = 0.03), as the 'collapse threshold' caused by the domination of *lasR* mutant. One replicate out of six did not follow this trend; in this case, no population collapse was observed, and the total cell numbers remained high throughout the experiment (Fig. S7*B*). The cause of this difference is currently under investigation, but the fact that it only occurred in one of the six replicates suggests that the WT in this particular replicate may have acquired *de novo* beneficial mutation(s), that could prevent invasion of *lasR* mutant, and these are likely to be non-social mutation(s).

Next, we analyzed long-term competitions in triple co-culture (WT, *pvdS*, and *lasR*; respectively 8:1:1) in iron-supplied casein medium (Fig. 3*B*, and Fig. S8). In this case, we observed an increase in *lasR* frequency, similar to that of

WT and *lasR* co-cultures seen in Fig. 3*A*, which was also accompanied by a drastic decrease in the overall population density. At day 10 of the propagation the six populations reached the collapse threshold. The frequencies of *pvdS* mutant varied between 4% and 15% throughout the duration of the experiment with no indication of any sustained increase (blue bars, Fig. 3*B*). This result is consistent with the predictions from the relative fitness measurements (Fig. 2*B*).

Then we propagated WT:*lasR* co-cultures in the medium with two constraints (Fig. 3*C*, and Fig. S9). In these propagations *lasR* mutant also increases in frequency throughout the first days, but at a slower pace than in iron-supplied medium. The total cell numbers remain high until days 10-12, but, as the *lasR* frequencies increase to about 80%, the density of the population decreases, reaching the collapse threshold by day 18.

Hence, in all the three scenarios described here, the dominance of *lasR* mutant is followed by a drastic population collapse due to the tragedy of the commons (Fig. 3 *A* – *C*).

## pvdS *mutant prevents the drastic population collapse caused by the invasion of* lasR *mutant*

Our short-term competitions revealed that the cheating ability of *lasR* is influenced by both abiotic and biotic conditions, as the presence of *pvdS* in the low iron conditions reduces the relative fitness of *lasR* mutant (Fig. 2*C*). Therefore, we investigated if, under low iron conditions, *pvdS* could protect a polymorphic population from the drastic population collapse caused by *lasR* invasion. Fig. 3*D* (and the individual replicates in Fig. S10) shows that in the propagation of triple co-cultures in iron-depleted casein medium, *lasR* cannot increase in frequency (it stays at approximately 3% throughout the experiment). In contrast, *pvdS* rapidly spreads during the first 12 days to an average frequency of 96% at day 18. Despite the *pvdS* domination, cell densities of the overall populations stay high. These indicate that, under these conditions, the presence of only 4% of pyoverdine producers in the population is enough to sustain the growth of the entire populations to levels similar to the WT mono-cultures. This interpretation is supported by the results shown in Fig. S11, representing growth yields of mixed cultures with different starting frequencies of *pvdS*.

Overall, the domination of *pvdS* mutant in the triple cultures with the two constraints has a remarkable effect on the outcome of the propagations in terms of the growth yields; *pvdS* domination prevents expansion of *lasR* and thus the drastic population collapse of the population, which occurs when *lasR* mutant dominates ($OD_{600}$=0.03, Fig. 3*A* – *C*). This occurs because, in this environment where both *lasR* mutant and WT are induced to produce pyoverdine*,* even though *lasR* mutant still increases in frequency in relation to the WT (Fig. S3*C*), it loses against *pvdS,* given the high relative fitness of *pvdS* against both WT and *lasR* in this medium (Fig. 2).

As a control, we also performed the long-term propagation experiments in media with no constraints. As expected, we did not observe any significant change in the population densities (Fig. S12).

***Manipulation of carbon or iron source availability can prevent or induce the collapse***

We reasoned that if strong ecological interactions dominate in long-term dynamics over *de novo* adaptive mutations, alterations of the abiotic factors in the triple cultures should modify the role of each mutant by changing the costs and benefits of the cooperative traits. Indeed, changing the carbon source from casein to CAA during the course of the propagation eliminated the behavior of *lasR* mutant as a cheater, and this environmental change was sufficient to protect the WT:*lasR* co-cultures from population collapse (Fig. 4*A*). Conversely, addition of iron to the iron-depleted casein medium (thus making it iron-supplied) reverts the expansion of *pvdS* mutant, favoring a consequent increase in *lasR* cheating capacity, ultimately causing the collapse of all the populations at day 18 (Fig. 4*B*). We confirmed that changes in final frequencies observed in Fig. 4*B* were not due to the high starting frequencies of *pvdS*; even though the selective advantage of *pvdS* is frequency dependent, this mutant is capable of cheating even at frequencies higher than 90% (Fig. S13).

Overall, these results show that by changing the roles of *lasR* and *pvdS* mutants, it was possible to revert the social and ecological dynamics of the populations in a very predictable and reproducible manner. The different consequences of these abiotic manipulations are related to the distinct characteristics of the two mutants studied here, *i. e.*, the tragedy of the

commons caused by invasion of *pvdS* causes a small drop in cell density while invasion of *lasR* leads to a much greater decrease in density.

### *A mathematical model of a 3-way public goods game explains the dynamics of the cheating mutants*

To further investigate the main general factors determining the dynamics of competitions among cooperators and cheaters, we built a simple mathematical model assuming that the fate of cooperators and cheaters is governed by the costs and the benefits of the cooperative traits. The model assumes that the cost (c) of a cooperative trait is lower than the benefit (b) associated with this trait (b>c>0). The model also assumes that the benefit provided by the cooperative trait is equal for the entire population, as it would be in the case of an equally accessible public good in a well-mixed environment. Spatial structure, diffusion or privatization, which would alter the benefit gained from the public good for cooperators and cheaters asymmetrically, were not considered in the model. The parameters used are described in Table 1.

#### a) Simple 3-way public goods model

We define the fitness of a cooperator and two cheaters mixed in an environment where both traits that these mutants cheat on are necessary as:

$$\omega_{coop} = \omega_0 + b_1 (1 - p_{ch1}) + b_2 (1 - p_{ch2}) - c_1 - c_2$$

$$\omega_{ch1} = \omega_0 + b_1 (1 - p_{ch1}) + b_2 (1 - p_{ch2}) - c_2$$

$$\omega_{ch2} = \omega_0 + b_1 (1 - p_{ch1}) + b_2 (1 - p_{ch2}) - c_1$$

As can be seen from the fitness definitions of these three players, the cheaters always have a higher fitness than the cooperator due to the costs ($c_1$ or $c_2$) saved. Assuming a homogeneous environment, and ignoring stochastic effects, the population changes according to the replicator equation system:

$$dp_{coop} / dt = p_{coop}(t) (\omega_{coop} - \bar{\omega}) = p_{coop}(t) \ (- c_1 p_{ch1}(t) - c_2 p_{ch2}(t))$$

$$dp_{ch1} / dt = p_{ch1}(t) \ (\omega_{ch1} - \bar{\omega}) = p_{ch1}(t) \ (c_1 (1 - p_{ch1}(t)) - c_2 p_{ch2}(t))$$

$$dp_{ch2} / dt = p_{ch2}(t) \ (\omega_{ch2} - \bar{\omega}) = p_{ch2}(t) \ (c_2 (1 - p_{ch2}(t)) - c_1 p_{ch1}(t))$$

The change in the mean fitness is given by:

$$\bar{\omega} = \Sigma_i \, p_i(t) \, \omega_i = \omega_0 + p_{coop}(t) \, \omega_{coop} + p_{ch1}(t) \, \omega_{ch1} + p_{ch2}(t) \, \omega_{ch2}$$

$$= \omega_0 + (b_1 - c_1) (1 - p_{ch1}(t)) + (b_2 - c_2) (1 - p_{ch2}(t))$$

Fig. 5*A* shows the predicted mean fitness and final frequencies of the different strains in the population assuming different $c_1/c_2$ ratios. It can be easily seen that cooperators will always go extinct, and that the two cheaters can only co-exist when $c_1 = c_2$.

Whenever $c_1 \neq c_2$, then the cheater that produces the more costly trait will lose. Therefore, the relation between $c_1$ and $c_2$ determines which cheater will dominate the population, independently of the benefits of these cooperative traits. On the other hand, the yield of the population will depend on, $\bar{\omega}$, which is affected by the difference between b and c values of each trait.

We simulated the four scenarios (Fig. S14 *A* – *D*) corresponding to the conditions in Fig. 3. In Fig. S14*A* and S14*C*, the cooperator for both traits (WT) and the cheater of the 1st cooperative trait compete ($p_{coop}(0) = 0.9$ and $p_{ch1}(0) = 0.1$), while the cheater of the 2nd cooperative trait is absent (hence $p_{ch2}(0)=0$). Whereas, in Fig. S14*B* and Fig. S14*D* all three strains compete ($p_{coop}(0) = 0.8$ and $p_{ch1}(0) = p_{ch2}(0) = 0.1$). In Fig. S14*A* and S14*B*, only the 1st cooperative trait is produced ($b_1 > c_1 > 0$, whereas $b_2 = c_2 = 0$) while in S14*C* and S14*D* both traits are expressed ($c_2 > c_1 > 0$ and $b_1 > b_2 > 0$). The $c_1/c_2$ ratio reflects the ratios of the relative fitnesses in Fig. 2*C* and 2*D*. The time scale of the simulations reflects the CCD as a more meaningful scale than days or numbers of generations (57, 58). CCD values were chosen according to the final number of cells measured in the competition in Fig. 2, where the CCD were significantly higher in iron-supplied casein medium than in iron-depleted casein medium for the same time period. $\omega_0$, $b_1$, and $b_2$ are chosen to reflect the growth yields in Fig. 1 and Fig. S1*B*.

The results of the model for the four scenarios (Fig. S14 *A*–*D*) resemble the experimental data, explaining changes in frequencies and the mean fitness observed reasonably well. However, this simple model always predicts complete fixation of the winning mutant (Fig. S14 *A*–*D*), and cannot explain the lack of fixation of the mutants observed experimentally with *lasR* (in Fig. 3 *A*–*C*) and *pvdS* (Fig. 3*D*). We experimentally tested whether fixation of the winning mutant could occur if the propagations were continued. Our results show that, *pvdS* mutant can reach fixation when co-cultured either with WT, or with WT and *lasR* mutant (Fig. S15*B* and Fig. S15*E*, respectively). However, *lasR* mutant fails to reach fixation (Fig. 6*A*). In the absence of *pvdS,* when we initiate

competitions with initial *lasR* frequencies similar to those at day 18 in Fig. 3*A*, *lasR* mutant fails to reach fixation and its frequencies stay around the levels similar to the ones observed in Fig. 3*A* after the populations collapse.

**b) Simple 3-way public goods model including quorum sensing**

Given that the *lasR* gene and elastase production are regulated via quorum sensing, we hypothesized that QS could be responsible for the lack of fixation of *lasR* mutant. QS regulation should reduce both the cost and the benefit of elastase production when the cooperators are below the QS threshold as the cells will not be producing it. We therefore modelled the effect of QS on fitness equations by assuming a Hill function where the cost ($c_1$) and benefit ($b_1$) of the 1$^{st}$ cooperative trait are sharply reduced when the frequency the cheater of the1$^{st}$ cooperative trait ($p_{ch1}$) reaches a given threshold value (th), as:

$$\omega_{coop} = \omega_0 + b_1 (1 - p_{ch1}) (1 / (1 + (p_{ch1} / th)^n)) + b_2 (1 - p_{ch2}) - c_1 (1 / (1 + (p_{ch1} / th)^n)) - c_2$$

$$\omega_{ch1} = \omega_0 + b_1 (1 - p_{ch1}) (1 / (1 + (p_{ch1} / th)^n)) + b_2 (1 - p_{ch2}) - c_2$$

$$\omega_{ch2} = \omega_0 + b_1 (1 - p_{ch1}) (1 / (1 + (p_{ch1} / th)^n)) + b_2 (1 - p_{ch2}) - c_1 (1 / (1 + (p_{ch1} / th)^n))$$

The change in the mean fitness is given by:

$$\bar{\omega} = \omega_0 + ((b_1 - c_1) (1 - p_{ch1}(t)) / (1 / (1 + (p_{ch1} / th)^n))) + (b_2 - c_2) (1 - p_{ch2}(t))$$

In this case, fixation of one mutant can only happen if $c_1 < c_2$. When $c_1 \geq c_2$, both cheaters can co-exist in the population (Fig. 5*B*).

As shown in Fig. 7, the results of the simulations of the modified model including QS for the four experimental conditions predict accurately both the frequency dynamics and the reduction in population size (assumed to be related to the mean fitness) as the cheaters spread. It is also now clear that by adding the QS regulation to the model the simulation predicts that *lasR* will not reach fixation.

To test experimentally if QS regulation prevents fixation of *lasR* in the WT:*lasR* competitions, we repeated the propagation experiment, shown in Fig. 6*A*, with the addition of the QS autoinducer AHLs ($3OC_{12}$-HSL) to the culture medium. Addition of AHLs abolishes the QS-dependent regulation of elastase by locking the LasR regulator on its ON state. With the addition of AHLs,

frequency of *lasR* mutant increases throughout the competitions until fixation (Fig. 6*B*), just like the model without QS had predicted (Fig. S14 *A* – *C*).

In supplementary material, we present other scenarios predicted by this model, which can be tested experimentally in the future (Fig. S16 – 19).

We conclude that quorum sensing regulation of production of a public good prevents full domination of the QS cheater, maintaining cooperation in populations. However, if the cheater which wins is affected in the production of a public good that is not regulated via QS (e.g. *pvdS*) this mutant can dominate the entire population. In summary, the results obtained from our mathematical model (Fig. 7) show that the dynamics observed in our propagation experiments in Fig. 3 can be explained by the relationship between the cost values of two orthogonal cooperative traits and a quorum threshold that regulates both costs and benefits of one of these traits.

## Discussion

The classical experimental approach in sociomicrobiology has been to study one trait and one constraint at a time. The simplicity of such an approach has substantially increased our understanding of the dynamics of cooperative and non-cooperative clones and revealed several mechanisms involved in the maintenance of cooperation (2, 4). The ability of *lasR* or *pvdS* mutants to behave as cheaters is well documented under these 'one constraint-one trait' laboratory settings. However, even though *lasR* and *pvdS* mutants are commonly isolated from bacterial populations colonizing CF lungs, population collapse due to the invasion by these mutants has not been seen in patients (38, 41).

Here, we established an experimental setup where WT cooperates in more than one trait: production of elastase and pyoverdine. Under this environment with two constraints, the *lasR* mutant is a cheater for elastase but, a cooperator for pyoverdine, whereas *pvdS* mutant does the opposite. In this environment, the advantage of *pvdS* mutant for not producing pyoverdine is higher than that of *lasR* for not producing elastase (Fig. 2*C* and Fig. 2*D*). As a consequence of the different costs associated with the different traits, in 3-way

competitions, *pvdS* causes a reduction in the relative fitness of *lasR* mutant and dominates the population. This domination of *pvdS* prevents the population from a potential drastic collapse caused by invasion of *lasR* mutants (compare Fig. 3*D* with Fig. 3 *A* – *C*). Although the tragedy of the commons due domination of *pvdS* mutant can also occur (Fig. S15), the consequent decrease in cell density, is much less drastic than the decrease in growth yields observed upon domination of *lasR* mutant (Fig. 1 and Fig. 3 *A* – *C*). This happens because the difference between the benefit and the cost of pyoverdine production is much smaller than that of elastase production.

The results from the 3-way competition demonstrate that by having more than one environmental constraint and more than one social mutant, a scenario likely to be closer to the conditions in nature (such as in the lungs of CF patients), the cheater for the trait with the highest cost is expected to dominate. The consequence of that domination for the population collapse will depend on the benefit-cost that such trait entails. Importantly, the degree of the population collapse caused by the tragedy of the commons can eventually have very different consequences for the host. In case of a trait whose difference in benefit to cost is high a drastic collapse on the density of the population caused by the cheater in that trait is expected. If drastic collapse in density takes place, clearance of the pathogen is more likely to occur, resulting in a higher benefit to the host. In contrast, if the mutant for the trait with a low benefit to cost difference (as for *pvdS*) wins, a weak collapse occurs, to the detriment of the host.

Altogether, our results provide support for a dynamic view of cooperation and cheating that is dependent on the genotypes and constraints present in the environment. We demonstrate how changes in the abiotic environment can make a social mutant to stop cheating on one trait while still cooperating on other traits also susceptible to cheating. Moreover, both the mathematical model and experimental results highlight the importance of the difference between costs of the difference traits for the population dynamics, and the difference between benefits and costs of each trait for the mean fitness of the population. Given the relationship between the costs, in a fluctuating environment, polymorphism of various mutants of cooperative traits, as it occurs in CF infections, is possible. Additionally, as shown here for *lasR* mutant,

quorum sensing regulation can also favor the maintenance of polymorphism, as such regulation alters the values of the cost and benefits of the traits.

A better understanding of the interactions in polymorphic bacterial populations in complex environments not only provides insights into key aspects of sociomicrobiology, but also can provide a theoretical framework for the development of new therapeutic strategies against bacterial populations where social mutants can invade. *P. aeruginosa* has been the focus of many clinical CF studies because *lasR* and *pvdS* mutants are repeatedly observed in the lungs of chronically infected patients (38, 41). Recently, it was suggested that controlled introduction of engineered *lasR* or *pvdS* cheaters into the lungs of CF patients infected by *P. aeruginosa* might decrease the bacterial population by inducing a tragedy of the commons (36, 59, 60). However, in the lungs, *P. aeruginosa* faces multiple constraints similar to the ones studied here: complex carbon sources and low iron concentrations. Thus, the order of the introduction of the cheaters, the composition of the bacterial population at the onset of the intervention, and the abiotic environmental conditions in the CF lungs are determinants for the ecological outcome of the population and the success of the intervention. For example, according to our results, introducing a *pvdS* mutant into a population containing *lasR* mutants in iron-limiting conditions might avert a drastic population collapse rather than triggering it. A study on the evolution of *P. aeruginosa* strains in the CF lungs showed that appearance of *lasR* mutations is followed by that of *pvdS* mutations (and other mutation affecting in iron metabolism) (41). This might explain why a drastic population collapse does not take place in the CF lungs. Our results suggest that a successful clearance of a *P. aeruginosa* infection in CF patients via triggering a tragedy of the commons can be achieved if the cheaters are introduced when the environmental constraints are limited to the specific trait that the cheater strain cheats on. Importantly, modifications of the environmental conditions can contribute to this effect. For instance, our results predict that when a *lasR* mutant is introduced, the supply of extra iron could accelerate the drastic collapse caused by the expansion of *lasR* mutant (Fig. 4*B*) and presumably addition of AHLs, by forcing WT to constitutively cooperate, can promote complete fixation of *lasR* mutants (Fig. 6*B*), therefore increasing the efficacy of this potential treatment. Our studies, do not take into account the effect of *pvdS,*

473 *lasR* double mutant (we found no evidence for emergence of double mutants
474 within the period of our experiments), which have the potential to occur *in vivo*
475 (41). The effect of such double mutants should be investigated in the future.
476 However, based on our results, we can speculate that double mutants should
477 accelerate the collapse of the population. Indeed, we have preliminary data
478 (data not shown) that in longer propagation experiment (in Fig. 3*D*), *de novo*
479 mutations can occur, which include *pvdS*, *lasR* double mutants. We further note
480 that, while our *pvdS* mutant does not show any advantage in iron-supplied
481 medium (Fig. 2*B*), some pyoverdine mutants in *Pseudomonas fluorescens* have
482 been reported to be better adapted even in environments where iron
483 concentration is not low and thus can be considered non-social mutations (46).
484 The observation of these potentially non-social mutants indicates that iron-
485 supplementation may sometimes fail as potential intervention for clearance,
486 highlighting the need for understanding the nature of these mutations and
487 changes in dynamics caused by them.

488 Collectively, our findings underline the need for including polymorphism
489 and multiple constraints in experimental studies and mathematical models
490 pertaining to cooperation in microbial populations. Our results demonstrate that
491 using experimental conditions that include more than one social trait can reveal
492 complex and dynamic social roles in bacterial populations as well as their
493 dependence on the environment. Understanding the dynamics of polymorphic
494 populations in these complex environments provides insights into social
495 interaction processes, expanding their relevance beyond sociomicrobiology, in
496 addition to providing knowledge important for the development of new
497 therapeutic tools.

498

499 **Materials and Methods**

500 **Bacterial strains, media and culture conditions.** We used *Pseudomonas*
501 *aeruginosa* WT strain PAO1 and its isogenic derivatives harboring a gentamycin
502 resistant gene inserted in either *pvdS* (*pvdS::Gm*) or *lasR* (*lasR::Gm*) (61). Iron-
503 supplied casein medium contains casein (Sigma, Ref: C8654) (1% w/v) as the
504 sole carbon and nitrogen sources salts (1.18 g $K_2HPO_4.3H_2O$ and 0.25 g

505 $MgSO_4.7H_2O$ per liter of $dH_2O$) and 50 µM of $FeCl_3$. Iron-depleted casein
506 medium is identical to the iron-supplied casein medium but instead of $FeCl_3$
507 supplementation, this medium contains 100 µg/ml of human apo-transferrin
508 (Sigma, T2036) and 20 mM sodium bicarbonate to deplete available iron and
509 induce pyoverdine production. The medium with no constraints contains the
510 same salt solutions as the other media, low iron CAA (BD, Ref: 223050) (1%
511 w/v) as the sole carbon source and 50 µM of $FeCl_3$. All cultures were incubated
512 at 37°C with aeration (240 rpm, New Brunswick E25/E25R Shaker) for the
513 incubation times indicated. Cell densities were estimated by measuring
514 absorbance (Abs) at 600 nm ($OD_{600}$) in a Thermo Spectronic Helios δ
515 spectrophotometer.

516 **Determination of genotypic frequencies.** Estimation of the frequencies of
517 each strain in the co-cultures was performed by scoring fluorescence and
518 colony morphology of colonies obtained from plating serial PBS dilutions of the
519 cultures. For each individual sample, three aliquots (of 50µl - 200µl, as
520 appropriated) were plated into LB agar plates, which were used as technical
521 replicates. Then, CFU/ml were calculated by scoring different colony
522 morphologies on each plates. A stereoscope (Zeiss Stereo Lumar V12) with a
523 CFP filter was used to distinguish pyoverdine producers, which are fluorescent,
524 from the non-fluorescent *pvdS* mutants (62, 63). *lasR* mutant colonies have
525 distinct colony morphology: smaller with smooth edges whereas elastase
526 producers are larger with rugged edges (63). To validate the phenotypic scoring
527 all colonies used to determine the frequency from day 18 of the propagation
528 experiments (Fig. 3*D*) were tested by PCR with primers for the *lasR* and *pvdS*
529 genes. The PCR data confirmed the phenotypic scoring with 100% accuracy.

530 **Competition experiments.** We propagated six replicates under four different
531 conditions (Fig. 3). Prior to start the competition experiments, all strains were
532 inoculated, from frozen stocks, in medium containing 1% (w/v) casein and 1%
533 (w/v) CAA in salts solution (same as in iron-supplied casein medium, described
534 above) for 36 hours at 37°C temperature with shaking (240 rpm). Cells were
535 then washed with PBS four times, to remove any residual extracellular factor.
536 Next after measuring cell densities ($OD_{600}$), cultures were normalized to $OD_{600}$ =
537 1.0 and used to inoculate the various media as described in the text and figures.

The different strains were diluted into fresh media, at different ratios as specified, to a starting initial $OD_{600}$ = 0.05. For short term competitions the relative frequencies were determined by plating an aliquot of each culture at the beginning of the experiment (t = 0), and after 48 hours of incubation. For long-term competitions, the relative frequencies were determined at t = 0, and thereafter every 48 hours before each passage. At the end of every 48 hours 1.5 µl of each culture was transferred to 1.5ml of fresh medium (bottle-neck of 1/1000).

**Statistical analysis.** Independent biological replicates were separately grown from the frozen stocks of each strain. Each experiment was performed at least twice, with three biological replicates, except in Fig. 2*A* where one experiment has only two biological replicates. Each figure (or figure panel) includes data from the biological replicates of at least two experiments. The sample size (N), corresponds to the total numbers of independent biological replicates in each figure panel and is provided in the corresponding figure legends. Relative fitness was used to determine the cheating capacity of each mutant. For both *lasR* and *pvdS* strains, the relative fitness (ω) was calculated as the frequency change over 48 hours relative to the rest of the strains in the mixture, using the following formula $\omega = f_{final}\,(1 - f_{initial}) / f_{initial}\,(1 - f_{final})$ where $f_{initial}$ is the mean of the initial proportion measured (as described above) at the beginning of the competitions while $f_{final}$ is the mean of the final proportions of the mutant after 48 hours of competition (62, 63). We used Mann-Whitney test which is a non-parametric test that does not account for normality and it is more suitable for the sample size used in each experiment ($5<N<20$). For multiple corrections, we used Kruskal-Wallis test with Dunn's correction. For all statistical analyses we used GraphPad Prism 6 software (http://www.graphpad.com/scientific-software/prism).

**ACKNOWLEDGEMENTS.** We thank Joana Amaro for technical assistance; João B. Xavier (Memorial Sloan Kettering), João Barroso-Batista, Rita Valente and Jessica Thompson for suggestions and helpful comments on the manuscript, Jan Engelstädter (The University of Queensland, Australia) for his help while building the mathematical model, and Kevin Foster (University of Oxford, UK) for sending the strains used in this work. This work is supported by

the Howard Hughes Medical Institute (International Early Career Scientist grant, HHMI 55007436). Roberto Balbontín is supported by European Research Council (ERC-2010-StG_20091118) and by Fundação para a Ciência e Tecnologia with a postdoctoral fellowship SFRH/BDP/109517/2015 Özhan Özkaya is supported by Fundação Calouste Gulbenkian with a Doctoral Fellowship 01/BD/13.

## References

1. Foster KR (2010) Social behaviour in microorganisms. *Social Behaviour: Genes, Ecology and Evolution*, eds Székely T, Moore AJ and Komdeur J, (Cambridge University Press, Cambridge), pp 331–356.
2. Bruger E, Waters C (2015) Sharing the sandbox: Evolutionary mechanisms that maintain bacterial cooperation. *F1000Research* 4(0):2–9.
3. Parsek MR, Greenberg EP (2005) Sociomicrobiology: The connections between quorum sensing and biofilms. *Trends Microbiol* 13(1):27–33.
4. Xavier JB (2016) Sociomicrobiology and Pathogenic Bacteria. *Microbiol Spectr* 4(3)(June):1–10.
5. Rankin DJ, Bargum K, Kokko H (2007) The tragedy of the commons in evolutionary biology. *Trends Ecol Evol* 22(12):643–651.
6. Hardin G (1968) The Tragedy of the Commons. *Science* 162(3859):1243–1248.
7. Waite AJ, Shou WY (2012) Adaptation to a new environment allows cooperators to purge cheaters stochastically. *Proc Natl Acad Sci U S A* 109(47):19079–19086.
8. MacLean RC (2008) The tragedy of the commons in microbial populations: insights from theoretical, comparative and experimental studies. *Heredity (Edinb)* 100(3):471–477.
9. Dandekar AA, Chugani S, Greenberg EP (2012) Bacterial Quorum Sensing and Metabolic Incentives to Cooperate. *Science* 338(6104):264–266.
10. Wang M, Schaefer AL, Dandekar AA, Greenberg EP (2015) Quorum sensing and policing of *Pseudomonas aeruginosa* social cheaters. *Proc*

*Natl Acad Sci* 112(7):2187–2191.

11. Asfahl KL, Walsh J, Gilbert K, Schuster M (2015) Non-social adaptation defers a tragedy of the commons in *Pseudomonas aeruginosa* quorum sensing. *ISME J* 9(8):1734–1746.
12. West SA, Griffin AS, Gardner A, Diggle SP (2006) Social evolution theory for microorganisms. *NatRevMicrobiol* 4(1740–1526):597–607.
13. Krakauer DC, Pagel M (1995) Spatial Structure and the Evolution of Honest Cost-Free Signalling. *Proc R Soc B Biol Sci* 260(1359):365–372.
14. Foster KR, Shaulsky G, Strassmann JE, Queller DC, Thompson CRL (2004) Pleiotropy as a mechanism to stabilize cooperation. *Nature* 431(7009):693–6.
15. Kreft J-U (2004) Biofilms promote altruism. *Microbiology* 150(8):2751–2760.
16. Lion S, Baalen M Van (2008) Self-structuring in spatial evolutionary ecology. *Ecol Lett* 11(3):277–295.
17. Kümmerli R, Griffin AS, West S a, Buckling A, Harrison F (2009) Viscous medium promotes cooperation in the pathogenic bacterium *Pseudomonas aeruginosa*. *Proc Biol Sci* 276(1672):3531–3538.
18. Nadell CD, Foster KR, Xavier JB (2010) Emergence of spatial structure in cell groups and the evolution of cooperation. *PLoS Comput Biol* 6(3):e1000716.
19. West SA, Winzer K, Gardner A, Diggle SP (2012) Quorum sensing and the confusion about diffusion. *Trends Microbiol* 20(12):586–594.
20. Dobay A, Bagheri HC, Messina A, Kümmerli R, Rankin DJ (2014) Interaction effects of cell diffusion, cell density and public goods properties on the evolution of cooperation in digital microbes. *J Evol Biol* 27(9):1869–1877.
21. Drescher K, Nadell CD, Stone HA, Wingreen NS, Bassler BL (2014) Solutions to the public goods dilemma in bacterial biofilms. *Curr Biol* 24(1):50–55.
22. Persat A, et al. (2015) The mechanical world of bacteria. *Cell* 161(5):988–997.
23. Banin E, Vasil ML, Greenberg EP (2005) Iron and *Pseudomonas*

*aeruginosa* biofilm formation. *Proc Natl Acad Sci U S A* 102(31):11076–81.

24. Harrison F, Buckling A (2009) Siderophore production and biofilm formation as linked social traits. *ISME J* 3(5):632–634.
25. Sandoz KM, Mitzimberg SM, Schuster M (2007) Social cheating in *Pseudomonas aeruginosa* quorum sensing. *Proc Natl Acad Sci U S A* 104(40):15876–15881.
26. Ross-Gillespie A, Dumas Z, Kümmerli R (2015) Evolutionary dynamics of interlinked public goods traits: An experimental study of siderophore production in *Pseudomonas aeruginosa*. *J Evol Biol* 28(1):29–39.
27. Wilder CN, Diggle SP, Schuster M (2011) Cooperation and cheating in *Pseudomonas aeruginosa*: the roles of the las, rhl and pqs quorum-sensing systems. *ISME J* 5(8):1332–43.
28. Friman V-P, Diggle SP, Buckling A (2013) Protist predation can favour cooperation within bacterial species. *Biol Lett* 9(5):20130548.
29. Wagner VE, Bushnell D, Passador L, Brooks AI, Iglewski BH (2003) Microarray Analysis of *Pseudomonas aeruginosa* Quorum-Sensing Regulons : Effects of Growth Phase and Environment. *J Bacteriol* 185(7):2080–2095.
30. Bachmann H, et al. (2013) Availability of public goods shapes the evolution of competing metabolic strategies. *Proc Natl Acad Sci U S A* 110(35):14302–7.
31. Kerr B, Neuhauser C, Bohannan BJM, Dean AM (2006) Local migration promotes competitive restraint in a host–pathogen “tragedy of the commons.” *Nature* 442(7098):75–78.
32. Hammarlund SP, Connelly BD, Dickinson KJ, Kerr B (2016) The evolution of cooperation by the Hankshaw effect. *Evolution (N Y)* 70(6):1376–1385.
33. Kümmerli R, et al. (2015) Co-evolutionary dynamics between public good producers and cheats in the bacterium *Pseudomonas aeruginosa*. *J Evol Biol* 28(12):2264–2274.
34. Kümmerli R, Brown SP (2010) Molecular and regulatory properties of a public good shape the evolution of cooperation. *Proc Natl Acad Sci U S A* 107(44):18921–6.

669 35. Xavier JB, Kim W, Foster KR (2011) A molecular mechanism that
670 stabilizes cooperative secretions in *Pseudomonas aeruginosa*. *Mol*
671 *Microbiol* 79(1):166–179.
672 36. Rumbaugh KP, et al. (2009) Quorum Sensing and the Social Evolution of
673 Bacterial Virulence. *Curr Biol* 19(4):341–345.
674 37. Czechowska K, McKeithen-Mead S, Al Moussawi K, Kazmierczak BI
675 (2014) Cheating by type 3 secretion system-negative *Pseudomonas*
676 *aeruginosa* during pulmonary infection. *Proc Natl Acad Sci U S A*
677 111(21):7801–7806.
678 38. Winstanley C, O'Brien S, Brockhurst MA (2016) *Pseudomonas*
679 *aeruginosa* Evolutionary Adaptation and Diversification in Cystic Fibrosis
680 Chronic Lung Infections. *Trends Microbiol* 24(5):327–337.
681 39. Cordero OX, Polz MF (2014) Explaining microbial genomic diversity in
682 light of evolutionary ecology. *Nat Rev Microbiol* 12(4):263–273.
683 40. Katzianer DS, Wang H, Carey RM, Zhu J (2015) Quorum non-sensing:
684 social cheating and deception in *Vibrio cholerae*. *Appl Environ Microbiol*
685 81(11):3856–3862.
686 41. Smith EE (2006) Genetic adaptation by *Pseudomonas aeruginosa* to the
687 airways of cystic fibrosis patients. *Proc Natl Acad Sci* 103(22):8487–8492.
688 42. Andersen SB, Marvig RL, Molin S, Krogh Johansen H, Griffin AS (2015)
689 Long-term social dynamics drive loss of function in pathogenic bacteria.
690 *Proc Natl Acad Sci* 112(34):10756–10761.
691 43. Sommer LM, Molin S, Johansen HK, Marvig RL (2015) Convergent
692 evolution and adaptation of *Pseudomonas aeruginosa* within patients with
693 cystic fibrosis. *Nat Genet* 47(1):57–65.
694 44. Nguyen AT, et al. (2014) Adaptation of iron homeostasis pathways by a
695 *Pseudomonas aeruginosa* pyoverdine mutant in the cystic fibrosis lung. *J*
696 *Bacteriol* 196(12):2265–2276.
697 45. Folkesson A, et al. (2012) Adaptation of *Pseudomonas aeruginosa* to the
698 cystic fibrosis airway: an evolutionary perspective. *Nat Rev Microbiol*
699 10(12):841–851.
700 46. Zhang X-X, Rainey PB (2013) Exploring the sociobiology of pyoverdin-
701 producing Pseudomonas. *Evolution* 67(11):3161–74.

47. Mellbye B, Schuster M (2014) Physiological framework for the regulation of quorum sensing-dependent public goods in *Pseudomonas aeruginosa*. *J Bacteriol* 196(6):1155–1164.

48. De Vos D, et al. (2001) Study of pyoverdine type and production by *Pseudomonas aeruginosa* isolated from cystic fibrosis patients: Prevalence of type II pyoverdine isolates and accumulation of pyoverdine-negative mutations. *Arch Microbiol* 175(5):384–388.

49. Visca P, Imperi F, Lamont IL (2007) Pyoverdine siderophores: from biogenesis to biosignificance. *Trends Microbiol* 15(1):22–30.

50. Cox CD, Adams P (1985) Siderophore activity of pyoverdin for *Pseudomonas aeruginosa*. *Infect Immun* 48(1):130–138.

51. Lamont IL, Beare PA, Ochsner U, Vasil AI, Vasil ML (2002) Siderophore-mediated signaling regulates virulence factor production in *Pseudomonas aeruginosa*. *Proc Natl Acad Sci U S A* 99(10):7072–7077.

52. Griffin AS, West S a, Buckling A (2004) Cooperation and competition in pathogenic bacteria. *Nature* 430(August):1024–1027.

53. Dumas Z, Kümmerli R (2012) Cost of cooperation rules selection for cheats in bacterial metapopulations. *J Evol Biol* 25(3):473–484.

54. Dumas Z, Ross-Gillespie A, Kümmerli R (2013) Switching between apparently redundant iron-uptake mechanisms benefits bacteria in changeable environments. *Proc Biol Sci* 280(1764):20131055.

55. Popat R, Harrison F, Mcnally L, Williams P, Diggle SP (2016) Environmental modification via a quorum sensing molecule influences the social landscape of siderophore production. *bioRxiv*. doi:10.1101/053918.

56. Lee J, Zhang L (2014) The hierarchy quorum sensing network in *Pseudomonas aeruginosa*. *Protein Cell* 6(1):26–41.

57. Luria S, Delbrück M (1943) Mutations of Bacteria from Virus Sensitivity to Virus Resistance. *Genetics* 28(6):491–511.

58. Lee DH, Feist AM, Barrett CL, Palsson B (2011) Cumulative number of cell divisions as a meaningful timescale for adaptive laboratory evolution of escherichia coli. *PLoS One* 6(10):1–8.

59. Brown SP, West SA, Diggle SP, Griffin AS (2009) Social evolution in micro-organisms and a Trojan horse approach to medical intervention

strategies. *Philos Trans R Soc Lond B Biol Sci* 364(1533):3157–3168.

60. Kümmerli R (2015) Cheat invasion causes bacterial trait loss in lung infections. *Proc Natl Acad Sci* 112(34):10577–10578.

61. Popat R, et al. (2012) Quorum-sensing and cheating in bacterial biofilms. *Proc Biol Sci* 279(1748):4765–4771.

62. Jiricny N, et al. (2010) Fitness correlates with the extent of cheating in a bacterium. *J Evol Biol* 23(4):738–747.

63. Ghoul M, West SA, Diggle SP, Griffin AS (2014) An experimental test of whether cheating is context dependent. *J Evol Biol* 27(3):551–556.

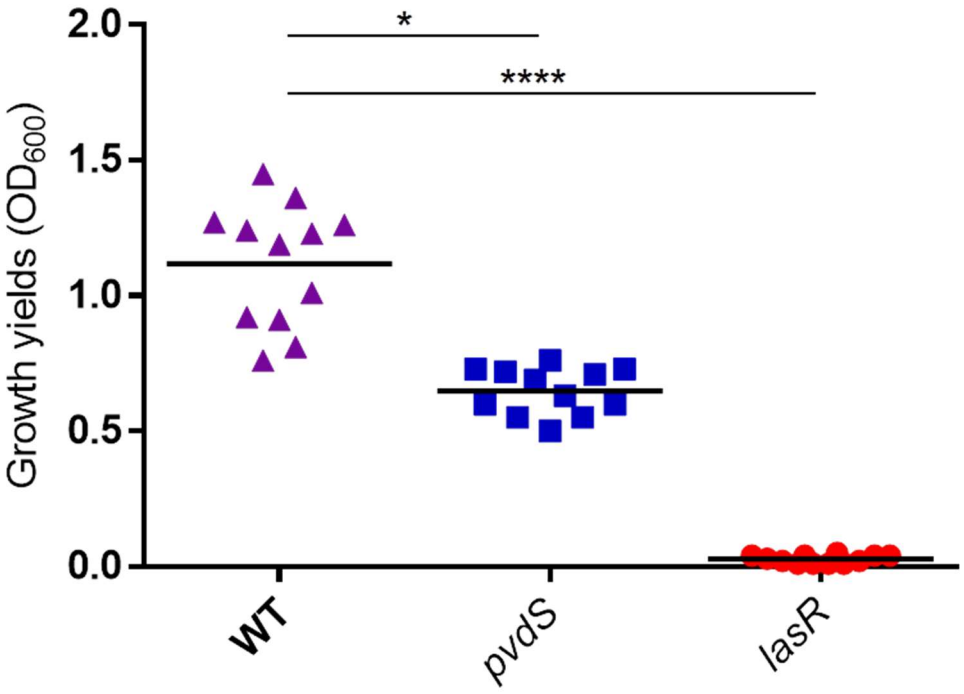


**Fig. 1.** Growth yields of *P. aeruginosa* monocultures in iron-depleted casein medium. WT (purple triangles), *pvdS* (blue squares) and *lasR* (red circles) mutant strains (horizontal lines show means of each group, Kruskal-Wallis test with Dunn's correction, WT-*pvdS* *=P=0.011, WT-*lasR* ****=P<$10^{-3}$, N=12).

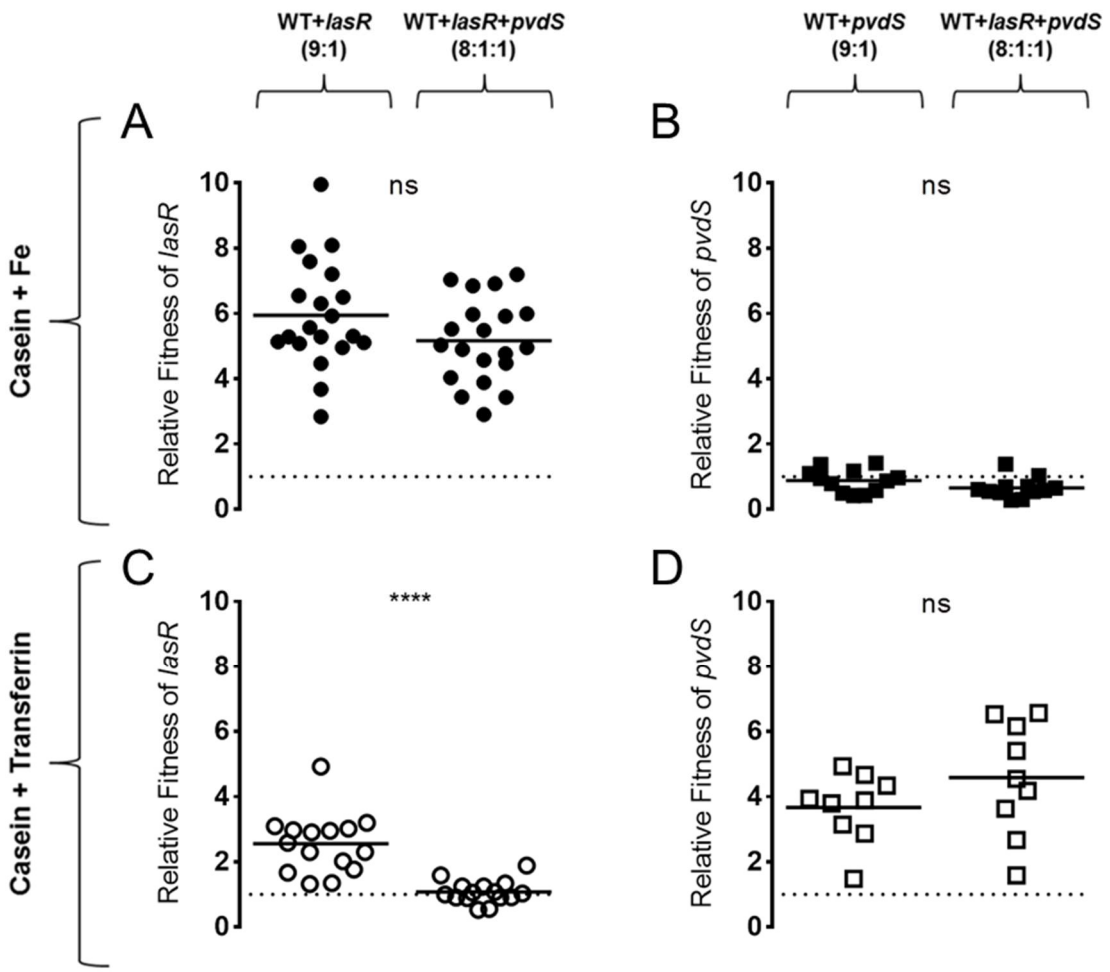


**Fig. 2.** Relative fitness of *lasR* or *pvdS* in iron-supplied or iron-depleted casein media in double or triple co-cultures. (*A*) Relative fitness of *lasR* (circles) in co-culture with WT, or with WT and *pvdS* in iron-supplied casein media (ns=not significant, P=0.1207, N=20). (*B*) Relative fitness of *pvdS* (squares) in co-culture with WT, or with WT and *lasR* in iron-supplied casein media (ns, P=0.1600, N=12). (*C*) and (*D*) same as in (*A*) and (*B*), respectively, but in iron-depleted casein media (****=P<$10^{-3}$, N=15 and ns, P=0.2581, N=9, for (C) and (D), respectively). Relative fitness of *lasR* or *pvdS* mutants is calculated in respect to all the other strains in the population. Relative fitness > 1 (above the dotted lines) indicate conditions where the frequency of the mutant increased in relation to the rest of the strains in the population during the competition. Initial ratios of the strains in each co-culture are 9:1 for WT:*lasR* and WT:*pvdS*, and 8:1:1 for WT:*pvdS*:*lasR*. Symbols indicate individual replicates and horizontal lines indicate the means of each group.

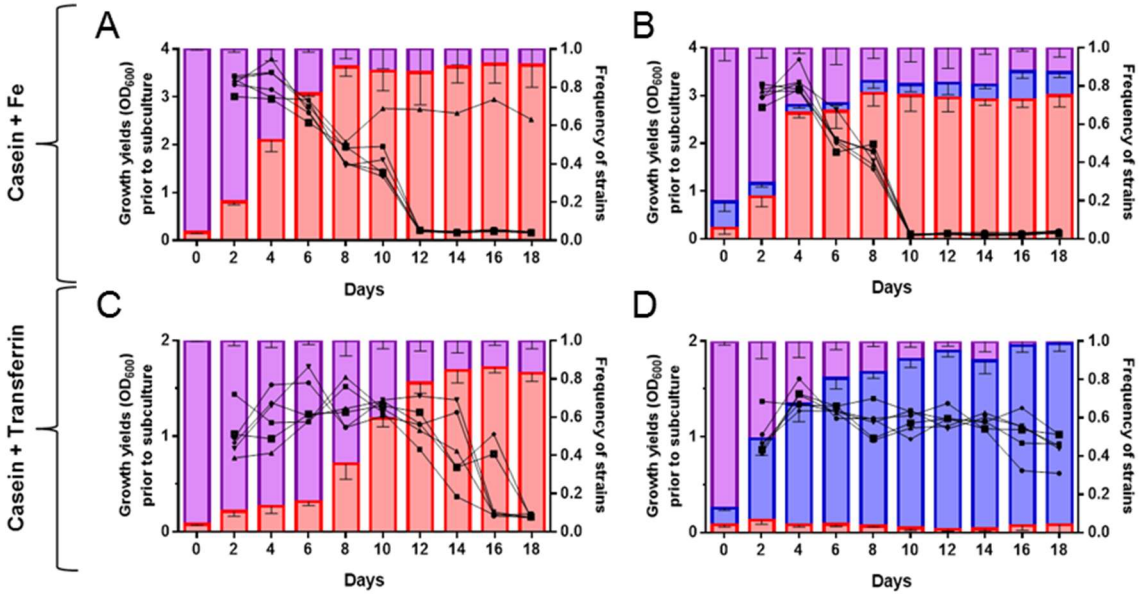


**Fig. 3.** Effects of abiotic and biotic factors on growth yields and strain composition of the population in long-term propagations. Left Y-axes show the $OD_{600}$ values prior to subculture; black symbols are the $OD_{600}$ values of 6 biological replicates tested for each condition (CFUs/ml are shown in Fig. S6). Right Y-axes show the frequencies of WT (purple), *lasR* (red), and *pvdS* (blue) mutants 48 hours after subculturing; data are shown as bars and represent the means of 6 biological replicates, error bars indicate SD. X-axes show the days of propagations to fresh media. (*A*) WT and *lasR* mutant co-cultures mixed at an initial frequency of 9:1 in iron-supplied casein media. (*B*) WT, *lasR* and *pvdS* mutants triple co-cultures mixed at initial an initial frequency of 8:1:1 in iron-supplied casein media. (*C*) and (*D*) same as in (*A*) and (*B*) but in iron-depleted casein media. Data from individual replicates are shown in Fig. S7 – 10.

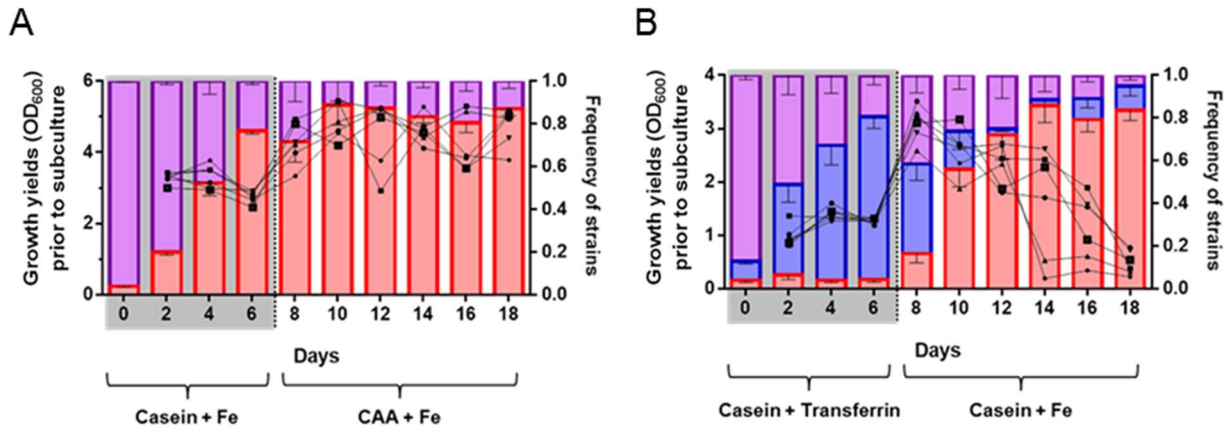


**Fig. 4**. Results of manipulations of abiotic conditions in long-term propagations. Aliquots of either the WT:*lasR* co-cultures propagated in iron-supplied casein media (Fig. 3*A*) or the WT:*lasR*:*pvdS* triple co-cultures propagated in iron-depleted casein media (Fig. 3*D*) for 6 days were transferred into either iron-supplied CAA medium or into iron-supplied casein medium, respectively. (*A*) Relief of complex carbon constraint by changing casein in iron-supplied casein medium to CAA, thus making it a medium with no constraints after the 6$^{th}$ day of the competitions (N=6, data from the first 6 days are from Fig. 3*A*). (*B*) Relief of low iron constraint by adding iron instead of iron depleting transferrin and changing iron-depleted casein medium into iron-supplied casein medium after the 6$^{th}$ day of the competitions (N=6, data from the first 6 days are from Fig. 3*D*). Legends as in Fig. 3.

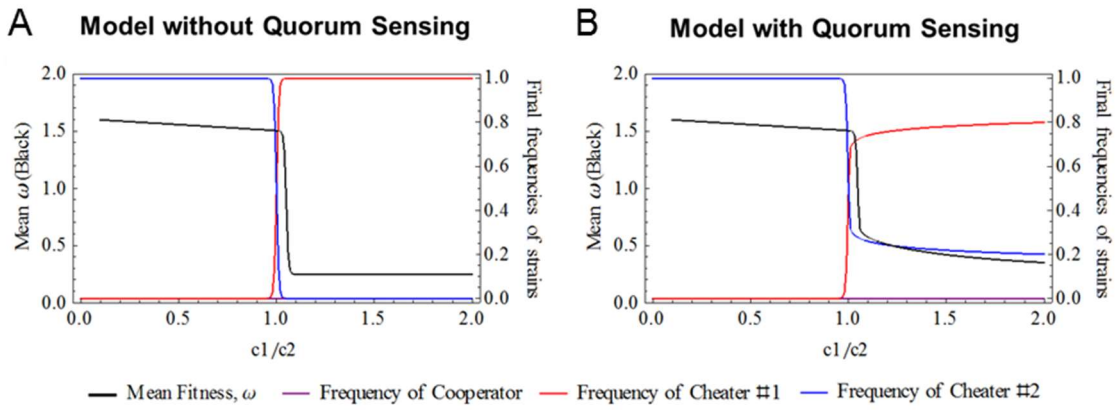


**Fig. 5.** Mathematical model for the final frequencies of the three strains in relation to the ratio of $c_1/c_2$. In Right-Y axes, frequencies of cooperator of both cooperative traits (**purple**), cheater of the 1st cooperative trait (**red**), and cheater of the 2nd cooperative trait (**blue**) in relation to the ratio of $c_1/c_2$ either without (***A***) or with the influence of quorum sensing (QS) regulation on the 1st cooperative trait (***B***). In Left-Y axes, the mean fitness, $\bar{\omega}$, is shown in **black**. The values given to the parameters of the simulations are: $p_{coop}(0)=0.8$, $p_{ch1}(0)=0.1$, $p_{ch2}(0)=0.1$, $0.001 \leq c_1 < 0.199$, $b_1=1.5$, $c_2=0.1$, $b_2=0.25$, $\omega_0=0.1$, time (as arbitrary CCD)=1800. In (*B*) the 1st cooperative trait is regulated by QS with n=30 and th=0.8.

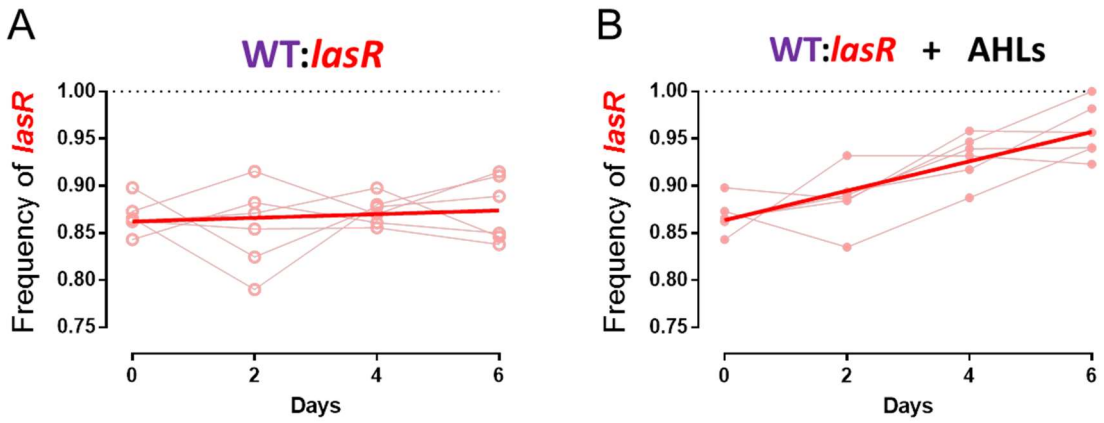


**Fig. 6.** Frequencies of *lasR* in propagations of WT:*lasR* co-cultures in iron-supplied casein media in the absence or presence of exogenously added AHLs ($3OC_{12}$-HSL). Initial frequency of 80-90% of *lasR* were used. Cultures were propagated throughout 6 days by passing the fresh media each 48 hours. **(*A*)** Frequency changes of *lasR* in WT:*lasR* co-cultures (red). **(*B*)** is the same as (*A*) but with 5μM AHLs ($3OC_{12}$-HSL) added to the media. Red lines indicate linear regressions of the data. Dotted lines represent 100% domination of *lasR*.

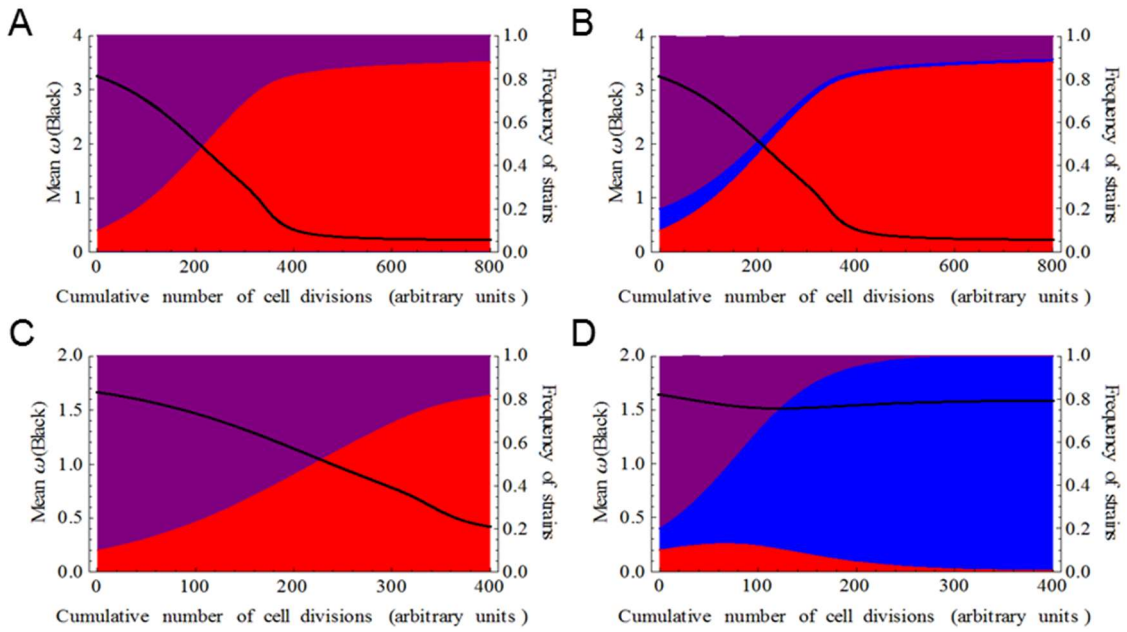


**Fig. 7.** Results of the mathematical model simulating the four scenarios in Fig. 3. Model includes quorum sensing regulation of the 1st cooperative trait ($b_1$ and $c_1$ are negatively regulated via a Hill equation as a function of the frequency of the mutant of this trait, $p_{ch1}$). Left Y-axes show $\bar{\omega}$, the mean fitness of the entire population which is a proxy of $OD_{600}$ or CFUs/ml values prior to subculture (black lines). Right Y-axes show the frequencies of $p_{coop}$ (e.g. WT, purple), $p_{ch1}$ (e.g. *lasR*, red) and $p_{ch2}$ (e.g. *pvdS,* blue). X-axes show the number of cell divisions as arbitrary units. The values that are given to the parameters of the simulations are: (*A*) $p_{coop}(0)$= 0.9, $p_{ch1}(0)$=0.1, $p_{ch2}(0)$=0, $c_1$=0.01, $b_1$=3.4, $c_2$=0, $b_2$=0, $\omega_0$=0.2, th=0.8, n=30; (*B*) $p_{coop}(0)$= 0.8, $p_{ch1}(0)$=0.1, $p_{ch2}(0)$=0.1, $c_1$=0.01, $b_1$=3.4, $c_2$=0, $b_2$=0, $\omega_0$=0.2, th=0.8, n=30; (*C*) $p_{coop}(0)$= 0.9, $p_{ch1}(0)$=0.1, $p_{ch2}(0)$=0 , $c_1$=0.01, $b_1$=1. 5, $c_2$=0.025, $b_2$=0.25, $\omega_0$=0.1, th=0.8, n=30; (*D*) $p_{coop}(0)$= 0.8, $p_{ch1}(0)$=0.1, $p_{ch2}(0)$=0.1, $c_1$=0.01, $b_1$=1.5, $c_2$=0.025, $b_2$=0.25, $\omega_0$=0.1, th=0.8, n=30.

**Table 1**: Parameters for the mathematical model for the 3-way public goods game.

| Symbols | Descriptions |
|---|---|
| $c_1$ | Cost of the 1st cooperative trait |
| $c_2$ | Cost of the 2nd cooperative trait |
| $b_1$ | Benefit gained from the 1st cooperative trait |
| $b_2$ | Benefit gained from the 2nd cooperative trait |
| $\omega_0$ | Fitness without the additional fitness effects of the cooperative traits (basal fitness) |
| $\omega_{coop}$ | Fitness of the cooperator of the both cooperative traits |
| $\omega_{ch1}$ | Fitness of the cheater of the 1st cooperative trait |
| $\omega_{ch2}$ | Fitness of the cheater of the 2nd cooperative trait |
| $\bar{\omega}$ | Mean fitness of the entire population (A proxy for $OD_{600}$ or CFUs/ml) |
| $p_{coop}$ | Frequency of the cooperator of the both cooperative traits in the entire population |
| $p_{ch1}$ | Frequency of the cheater of the 1st cooperative trait in the entire population |
| $p_{ch2}$ | Frequency of the cheater of the 2nd cooperative trait in the entire population |
| | **Parameters considered only in the model with QS** |
| th | Quorum threshold (as a function of the non-QS strain frequency) |
| n | Hill coefficient for the slope of the inhibition of the QS-regulated public good |

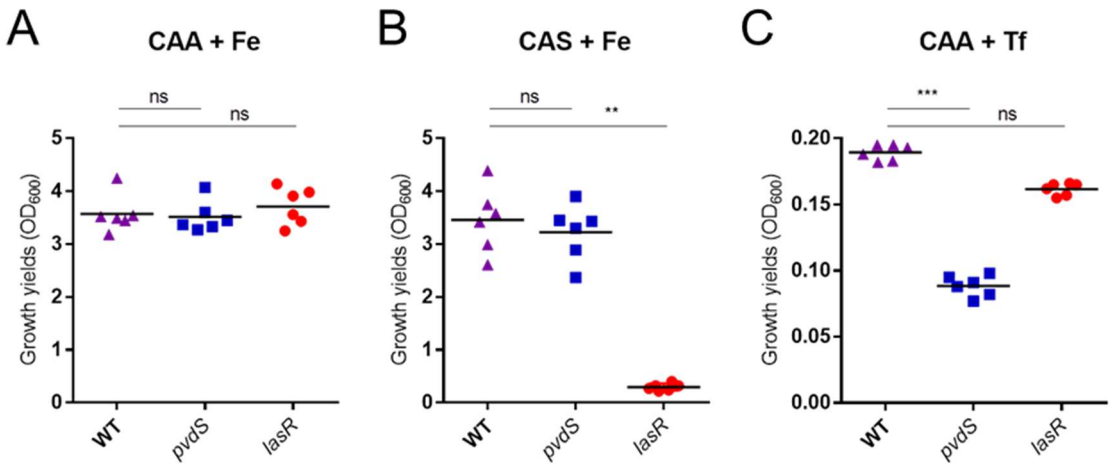


**Fig. S1:** Growth yields ($OD_{600}$) of WT (purple triangles), *pvdS* (blue squares) and *lasR* (red circles) strains of *P. aeruginosa* monocultures after 48 hours of incubation in various media. **(*A*)** WT, *pvdS*, and *lasR* growth yields in iron-supplied casamino acids (CAA) medium (Kruskal-Wallis test with Dunn's correction, WT-*pvdS* ns=not significant P>0.9999, WT-*lasR* ns=not significant P>0.9999, N=6). **(*B*)** WT, *pvdS,* and *lasR* growth yields in iron-supplied casein medium (Kruskal-Wallis test with Dunn's correction, WT-*pvdS* ns=not significant P>0.9999, WT-*lasR* **=P=0.0034, N=6). **(*C*)** WT, *pvdS,* and *lasR* growth yields in iron-depleted CAA medium. (Kruskal-Wallis test with Dunn's correction, WT-*pvdS* ***=P=0.0002, WT-*lasR* ns=not significant P=0.1027, N=6).

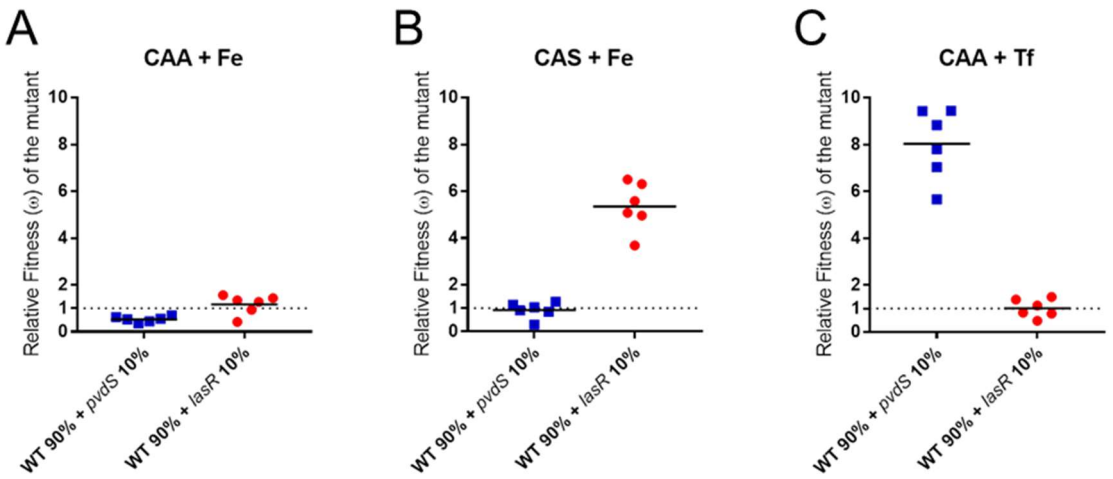


**Fig. S2:** Relative fitness of the mutants in co-cultures with WT with initial frequencies 9:1 WT:*pvdS* (blue squares) or 9:1 WT:*lasR* (red circles) after 48 hours of incubation in various media. **(*A*)** Relative fitness of *pvdS* and *lasR* in iron-supplied CAA medium (N=6). **(*B*)** Relative fitness of *pvdS* and *lasR* in iron-supplied casein medium (N=6). **(*C*)** Relative fitness of *pvdS* and *lasR* in iron-depleted CAA medium (N=6). Dotted lines indicate no change in relative fitness (relative fitness=1).

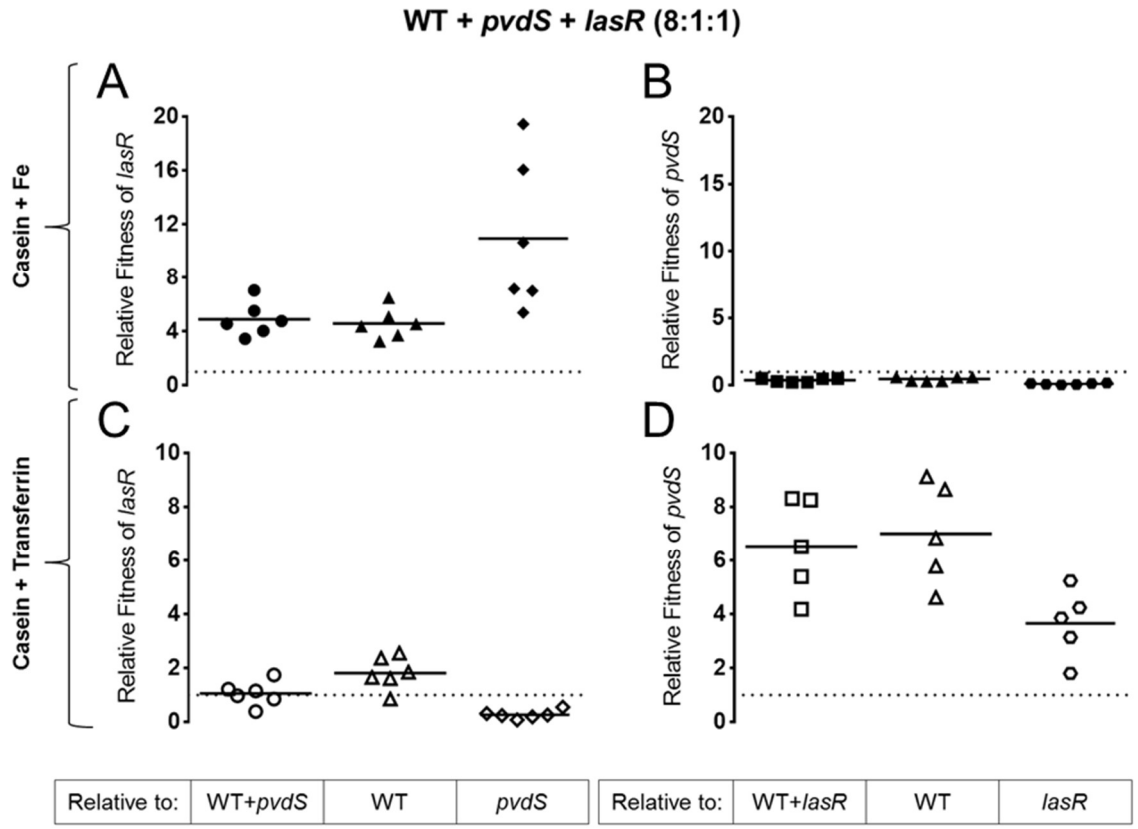


**Fig. S3.** Fitnesses of *lasR* and *pvdS* relative to the rest of the population, or to WT, or the other mutant in iron-supplied or iron-depleted casein media in WT:*pvdS*:*lasR* triple co-culture with the initial frequencies 8:1:1 (Data from Fig. 2). **(*A*)** Fitness of *lasR*, in iron-supplied casein media, relative to WT:*pvdS* (circles), WT (triangles) and *pvdS* (diamonds). **(*B*)** Fitness of *pvdS*, in iron-supplied casein media, relative to WT:*lasR* (squares), WT (filled) and *lasR* (hexagons). **(*C*)** and **(*D*)** same as in (*A*) and (*B*) (but with empty symbols), respectively, but in iron-depleted casein media. Symbols indicate individual replicates and horizontal lines indicate the means of each group. Dotted lines indicate no change in relative fitness (relative fitness=1).

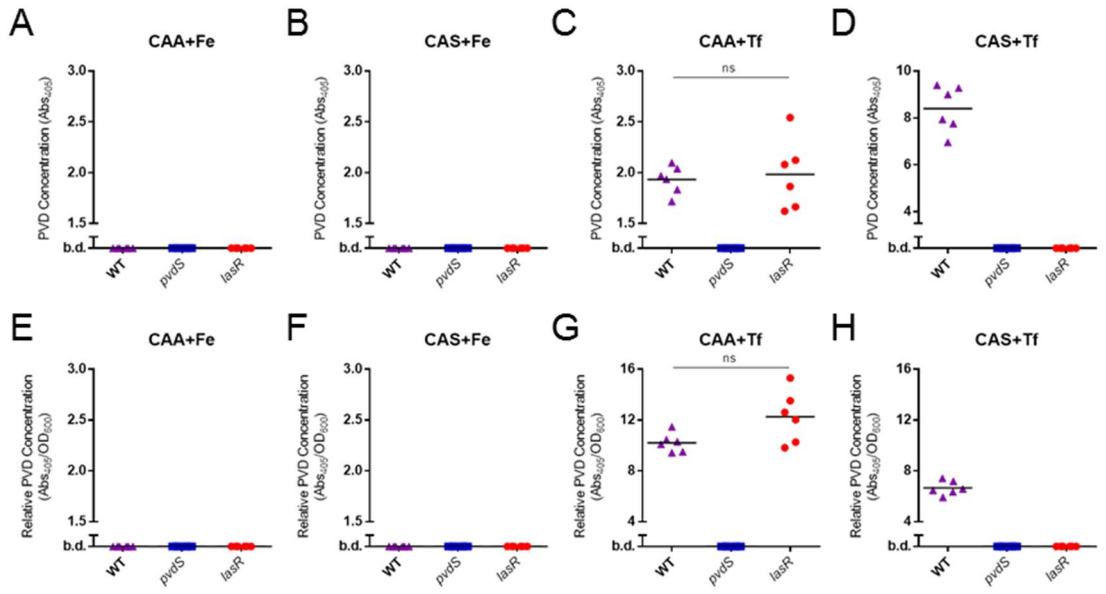


**Fig. S4.** Total ($Abs_{405}$) and relative ($Abs_{405}/OD_{600}$) pyoverdine (PVD) concentrations of WT, *pvdS*, and *lasR* monocultures after 48 hours of incubation in various media. Total PVD concentrations ($Abs_{405}$), **(*A*)** in iron-supplied CAA medium, **(*B*)** in iron-supplied casein medium, **(*C*)** in iron-depleted CAA medium, **(*D*)** in iron-depleted casein medium**.** Relative PVD concentrations ($Abs_{405}/OD_{600}$), **(*E*)** in iron-supplied CAA medium, **(*F*)** in iron-supplied casein medium, **(*G*)** in iron-depleted CAA medium, **(*H*)** in iron-depleted casein medium. (Comparisons are done via Mann-Whitney test; ns=not significant, P>0.05; for all experiments N=6; b.d.: below detection). **Methodology.** PVD concentration measurements are done after 48 hours of growth in 37ºC shaker by centrifuging the cells at 14000 r.p.m. for 4 minutes (Eppendorf Centrifuge 5418) and collecting the supernatant, measuring their absorbance at 405nm ($Abs_{405}$) in optical cuvettes as 1:10 dilutions with PBS solutions in a Thermo Spectronic Helios δ spectrophotometer.

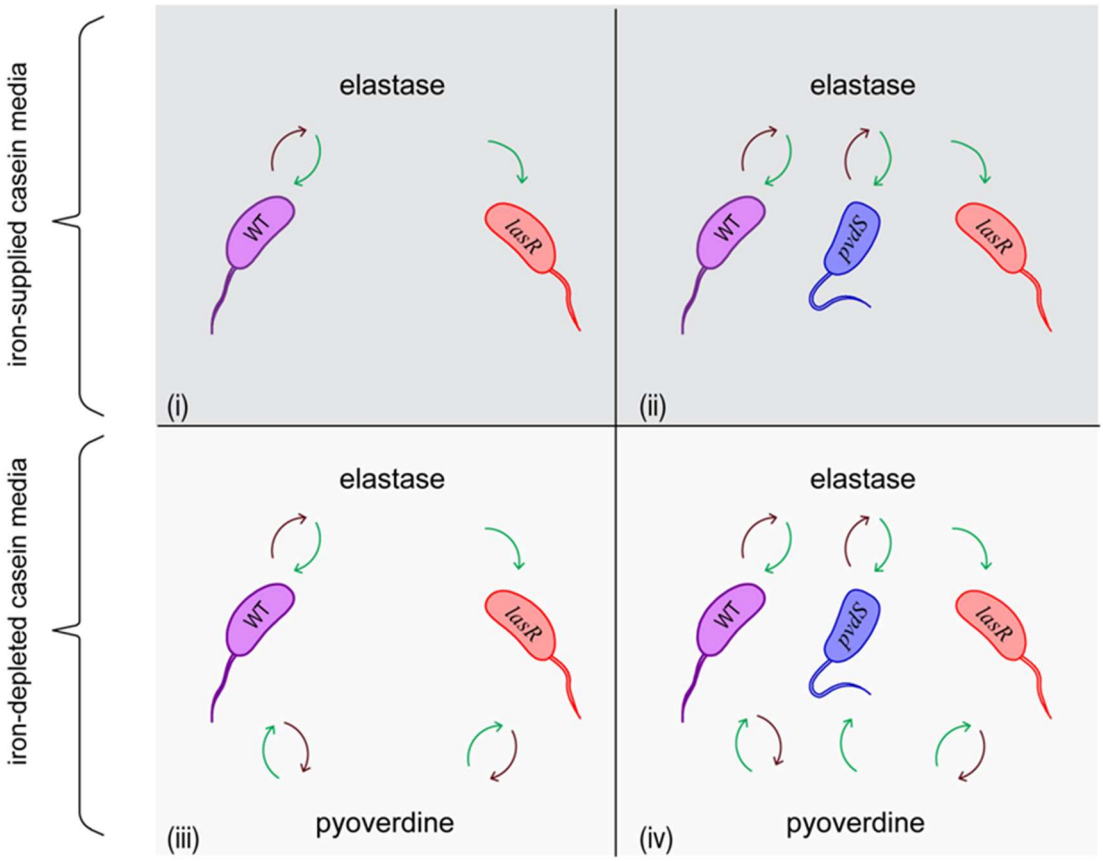


**Fig. S5.** Four scenarios representing the environmental constraints and population compositions tested. **i)** double co-culture in iron-supplied casein medium (WT and one mutant, under one environmental constraint); **ii)** triple co-culture in iron-supplied casein medium (WT and two mutants, under one environmental constraint); **iii)** double co-culture in iron-depleted casein medium (WT and one mutant, under two environmental constraints); **iv)** triple co-culture in iron-depleted casein medium (WT and two mutants, under two environmental constraints). Dark-red arrows indicate a paid cost for the production of elastase and/or pyoverdine, and the green arrows indicate a benefit from these behaviors. Dark-grey backgrounds indicate optimal iron concentrations; light-grey backgrounds indicate depleted iron concentrations in the media.

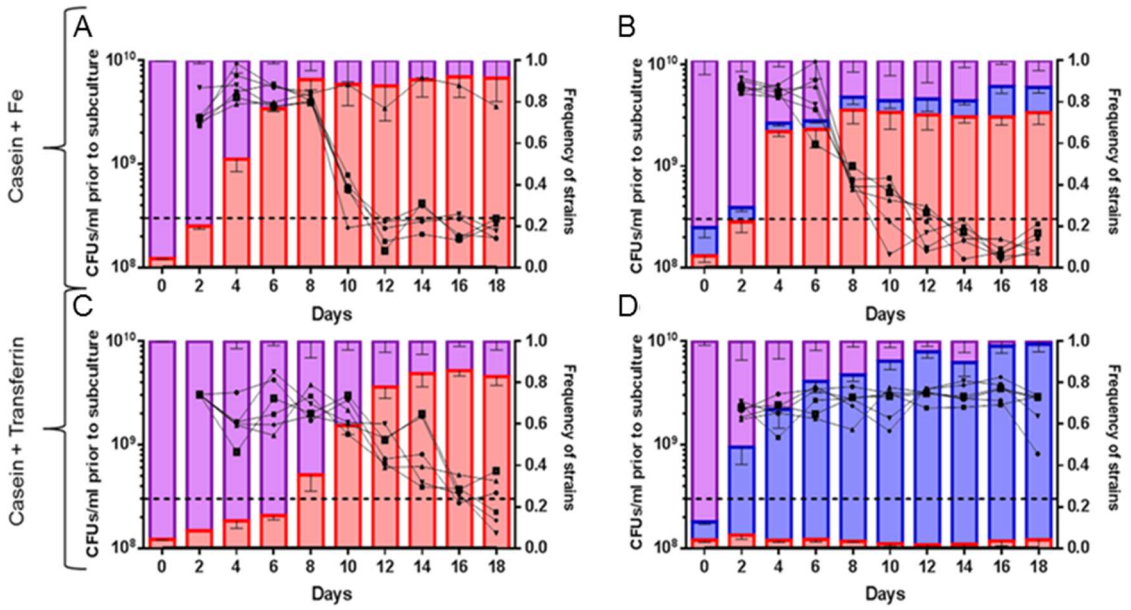


**Fig. S6.** Data from the experiments shown in Fig. 3 with the growth yields prior to subculture, shown as CFUs/ml. Dash lines indicate the approximate monoculture growth yields of *lasR* monoculture ($3x10^8$ CFUs/ml).

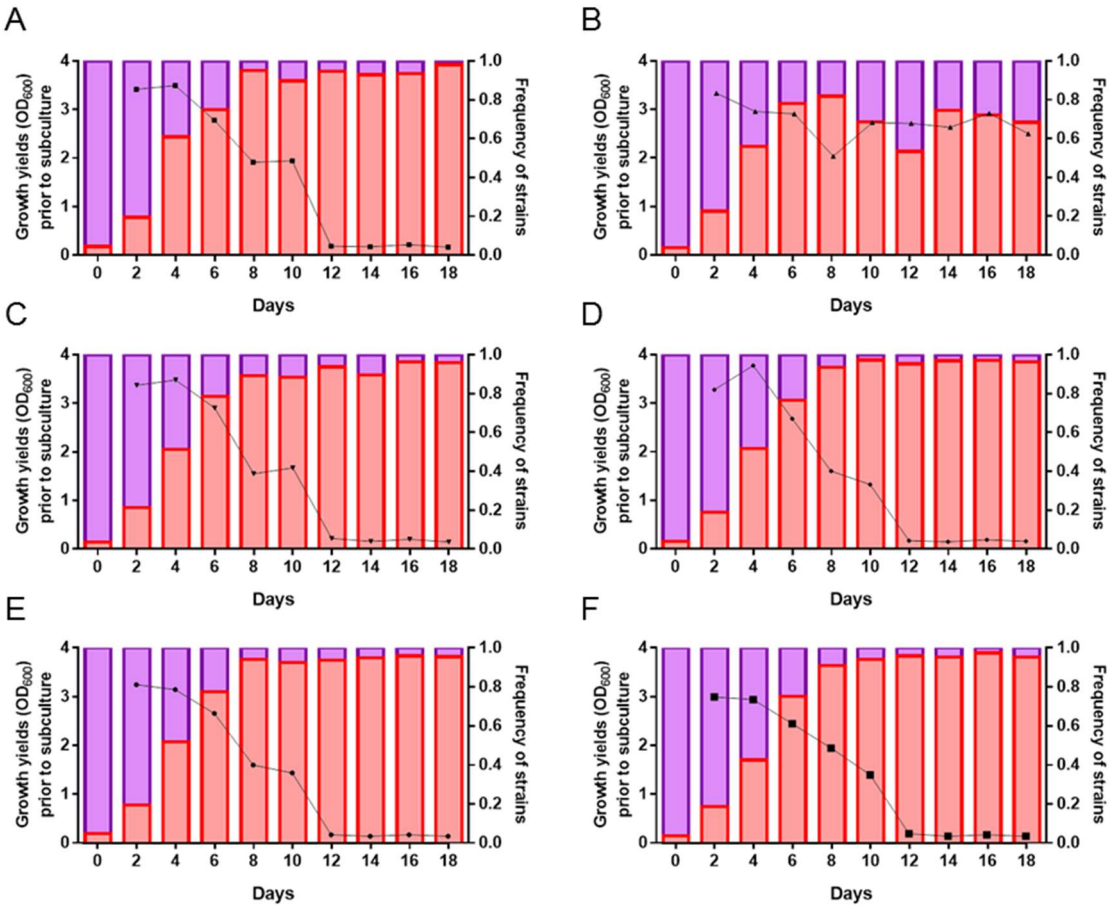


**Fig. S7.** Individual biological replicates from the Fig. 3*A*. WT:*lasR* populations, which are co-cultured with initial frequencies of 9:1, in iron-supplied casein media. 'X' axes show the days of propagations to fresh media. Left 'Y' axes show the growth yields ($OD_{600}$), prior to subculture; data shown as black lines are the growth yields ($OD_{600}$) of the cultures measured at the late stationary phase (48 hour after the inoculation) values. Right 'Y' axes show the frequencies of WT (purple) and *lasR* (red).

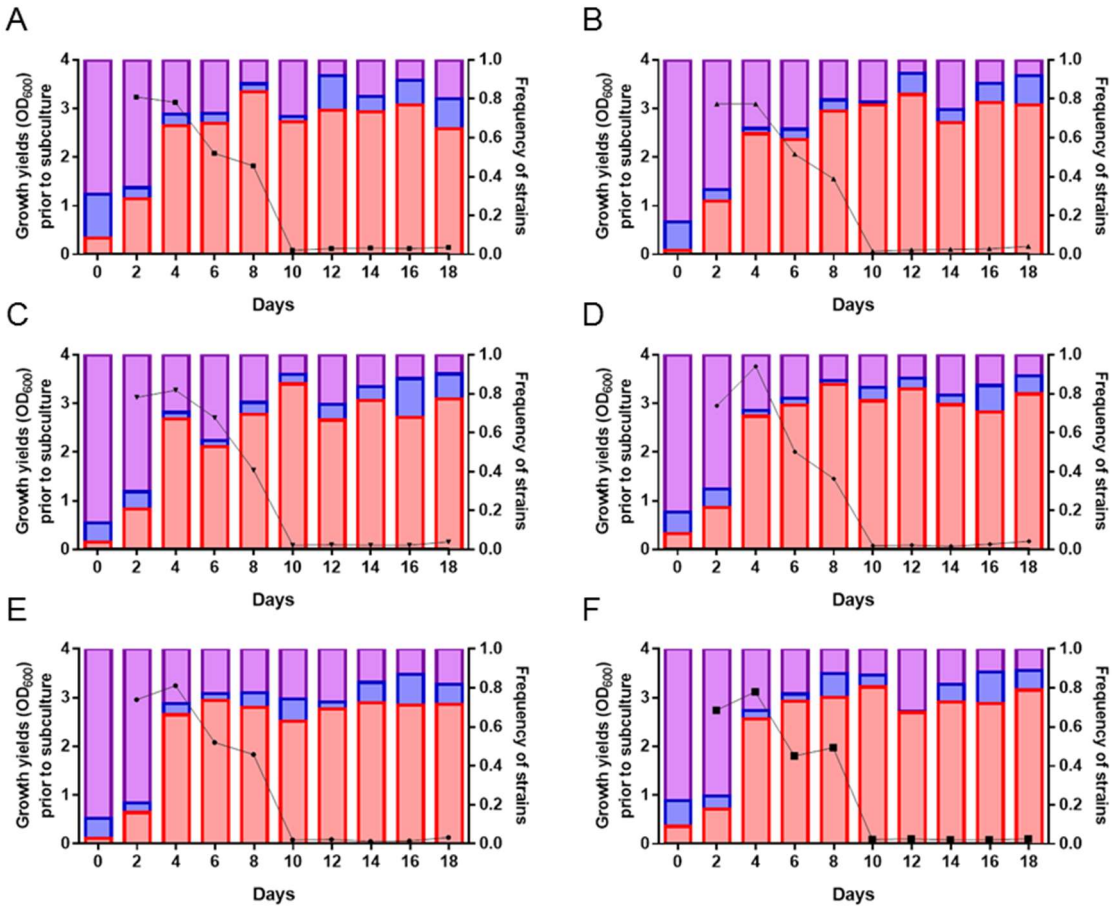


**Fig. S8.** Individual biological replicates from the Fig. 3*B*. WT:*lasR*:*pvdS* populations, which are co-cultured with initial frequencies of 8:1:1, in iron-supplied casein media.. 'X' axes show the days of propagations to fresh media. Left 'Y' axes show the growth yields ($OD_{600}$) prior to subculture; data shown as black lines are the growth yields ($OD_{600}$) of the cultures measured at the late stationary phase (48 hour after the inoculation) values. Right 'Y' axes show the frequencies of WT (purple), *pvdS* (blue), and *lasR* (red).

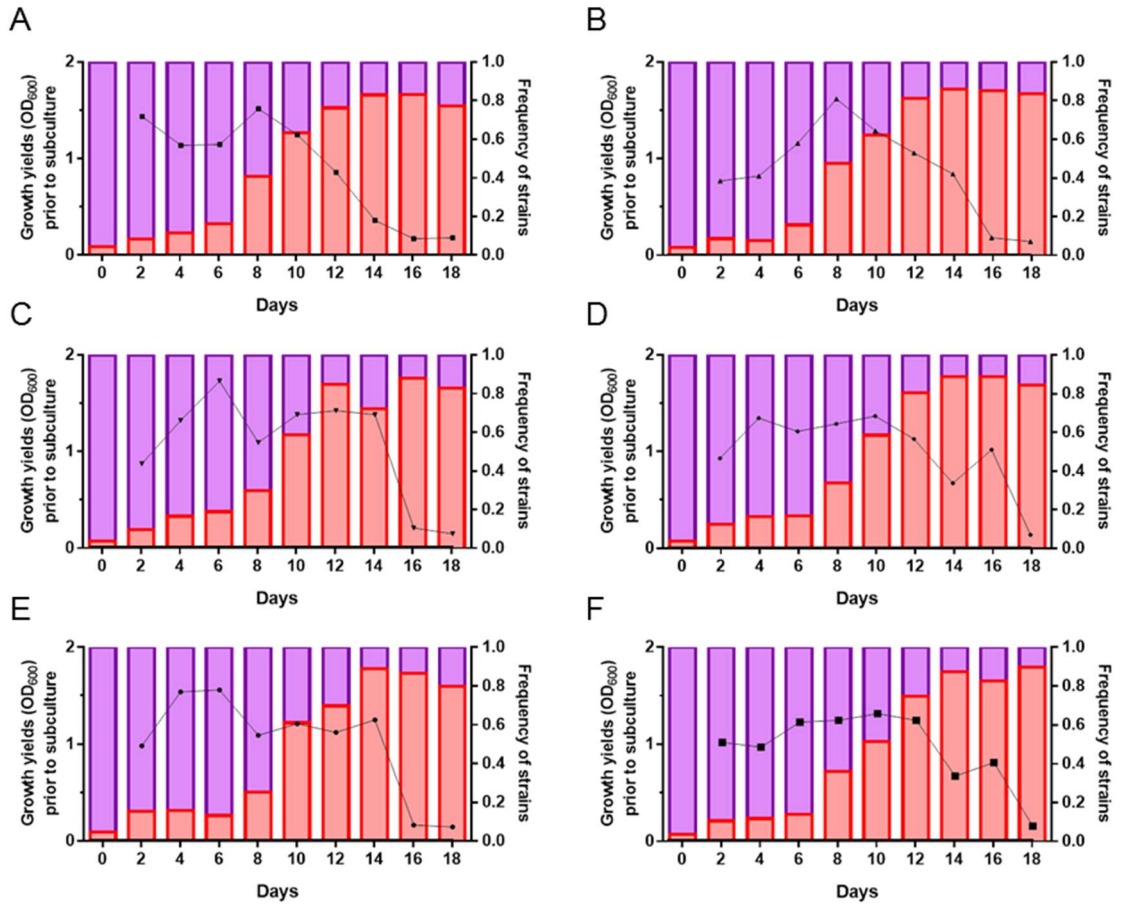


**Fig. S9:** Individual biological replicate from the Fig. 3*C*. WT:*lasR* populations, which are co-cultured with initial frequencies of 9:1, in iron-depleted casein media. 'X' axes show the days of propagations to fresh media. Left 'Y' axes show the growth yields ($OD_{600}$) prior to subculture; data shown as black lines are the growth yields ($OD_{600}$) of the cultures measured at the late stationary phase (48 hour after the inoculation) values. Right 'Y' axes show the frequencies of WT (purple) and *lasR* (red).

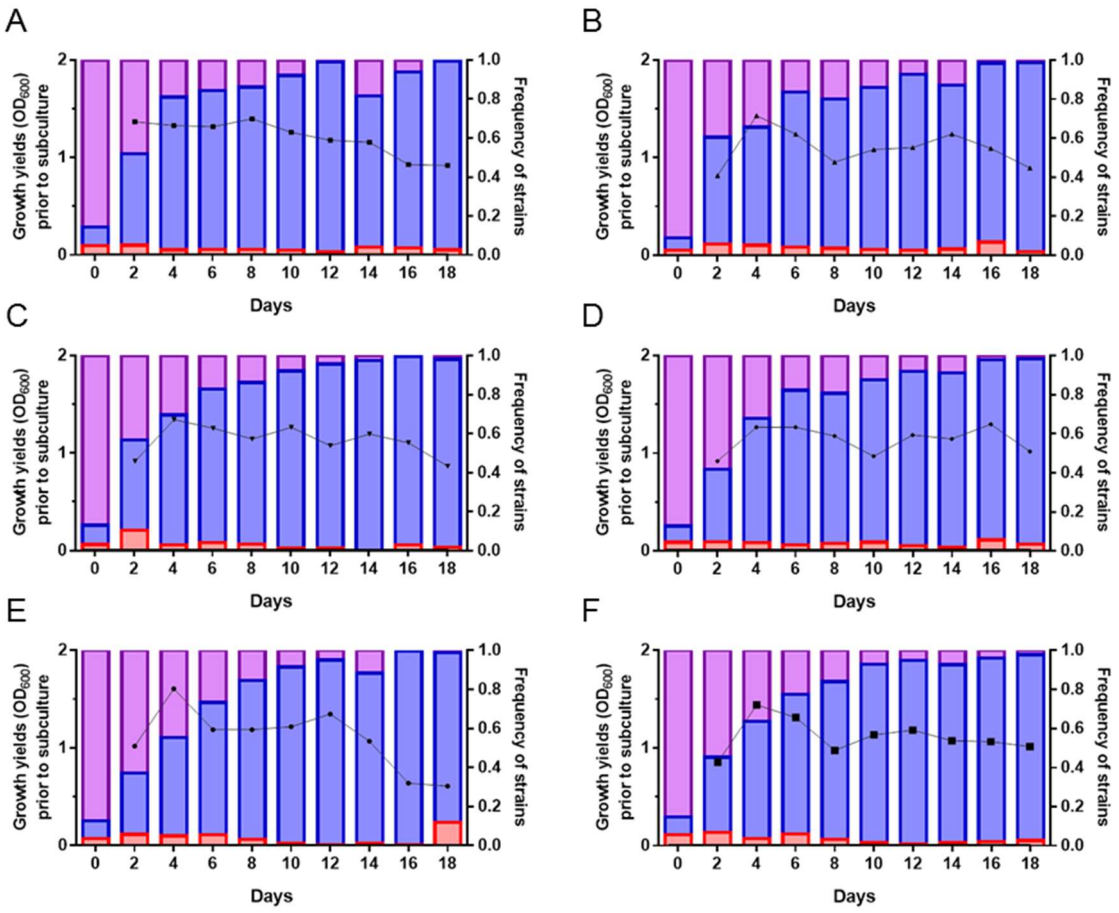


**Fig. S10.** Individual biological replicates from the Fig. 3*D*. WT:*lasR*:*pvdS* populations, which are co-cultured with initial frequencies of 8:1:1, in iron-depleted casein media. 'X' axes show the days of propagations to fresh media. Left 'Y' axes show the growth yields ($OD_{600}$) prior to subculture; data shown as black lines are the growth yields ($OD_{600}$) of the cultures measured at the late stationary phase (48 hour after the inoculation) values. Right 'Y' axes show the frequencies of WT (purple), *pvdS* (blue), and *lasR* (red).

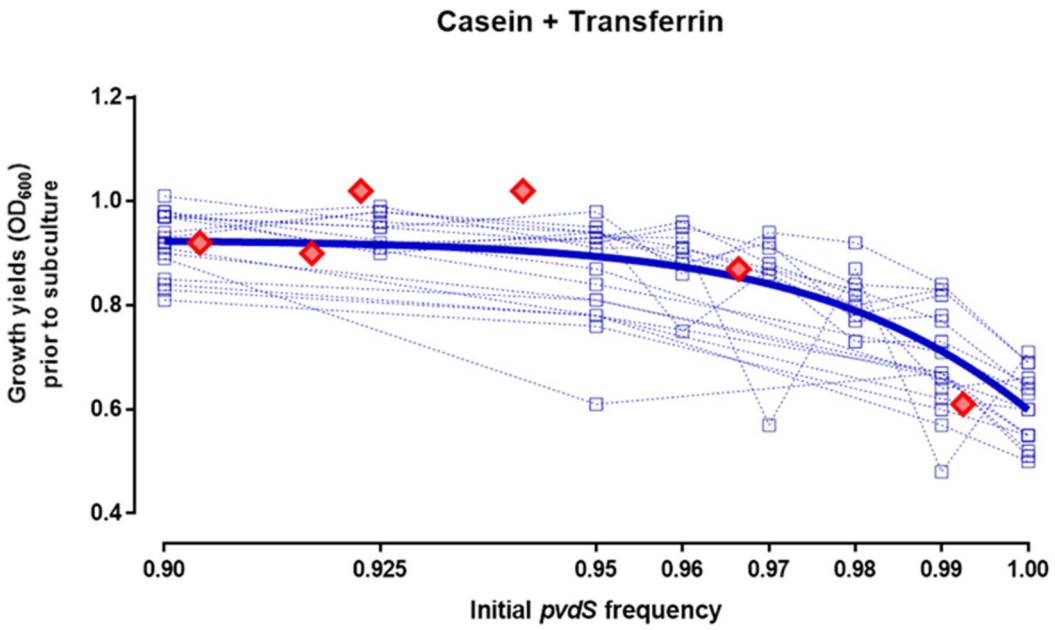


**Fig. S11.** Effect of the initial frequencies of *pvdS* mutant in the co-cultures with WT, on the overall growth yields of the population. Each blue square represents one short term competition (48 hours) in iron-depleted casein media. Initial frequencies of *pvdS* are shown in the 'X' axis (curve indicates the log regression of these short term competitions). Red diamonds show the $OD_{600}$ measurements and matching inoculum frequencies of *pvdS* mutant from different co-cultures of the 18$^{th}$ day of the experiment shown in Fig. 3*D* ($OD_{600}$ of the cultures with 3% WT and 97% *pvdS* vs. 100% WT, P=0.1316; and $OD_{600}$ of the cultures with 2% WT and 98% *pvdS* vs 100% WT, P<0.05).

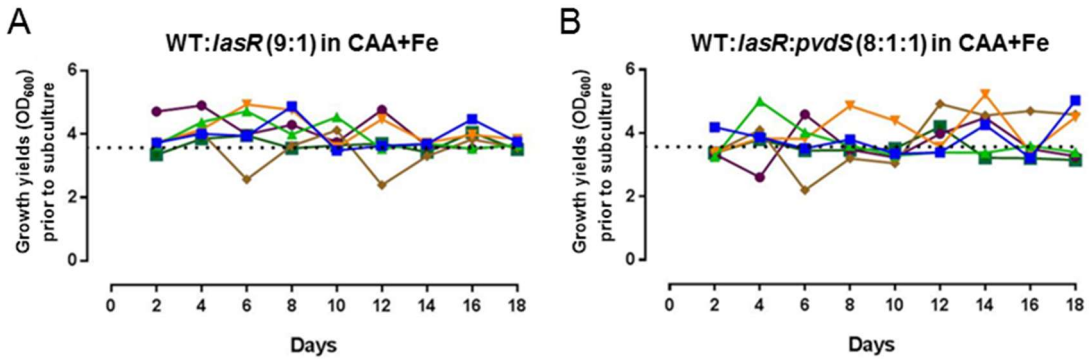


**Fig. S12.** Propagations of *P. aeruginosa* cultures in a medium with no constraints. **(*A*)** WT and *lasR* co-culture initially mixed (9:1) in iron-supplied CAA media. **(*B*)** WT, *pvdS* and *lasR* co-culture initially mixed (8:1:1) in iron-supplied CAA media. 'X' axes show the days of propagations to fresh media. 'Y' Axes show the growth yields as $OD_{600}$ prior to subculture, each colored line indicates one propagated culture (N=6), dash lines indicate the monoculture WT growth yields in the same medium (mean=3.57, ±SD=0.357, N=6) as shown in Fig. S1*A*.

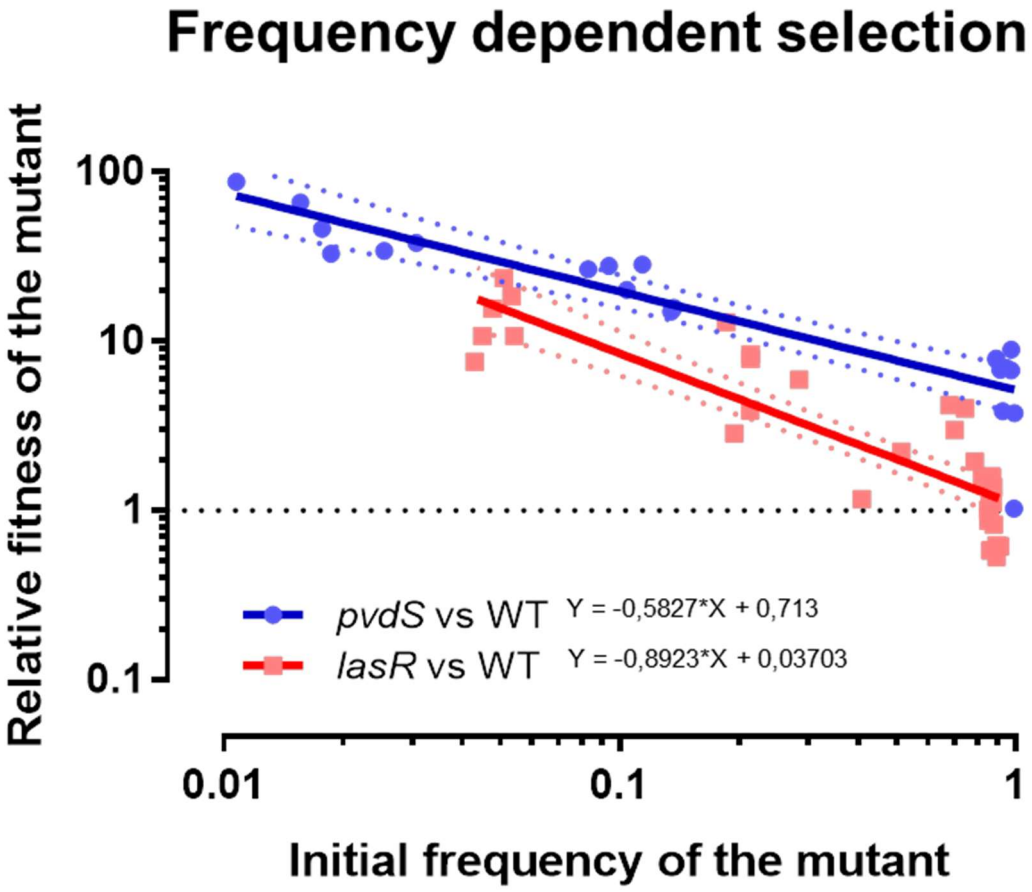


**Fig. S13.** Frequency-dependent selection for *pvdS* (blue circles) and *lasR* (red squares) when in co-culture with WT in iron-depleted or iron-supplied casein media for *pvdS* or *lasR,* respectively. 'X' axis shows the frequencies of *pvdS* or *lasR* in the beginning of the competition with WT. 'Y' axis shows the relative fitness values of *pvdS* or *lasR* over WT after 48h of incubation. Lines indicate linear regressions; slopes of the lines are shown on the figure (Comparison of the lines: F=8,525, DFn=1, DFd=52, **=P=0,0052; the lines are significantly different). Red and blue dots indicate the 95% confidence intervals of the corresponding lines. The gray dotted line indicates no change in relative fitness (no cheating, relative fitness=1).

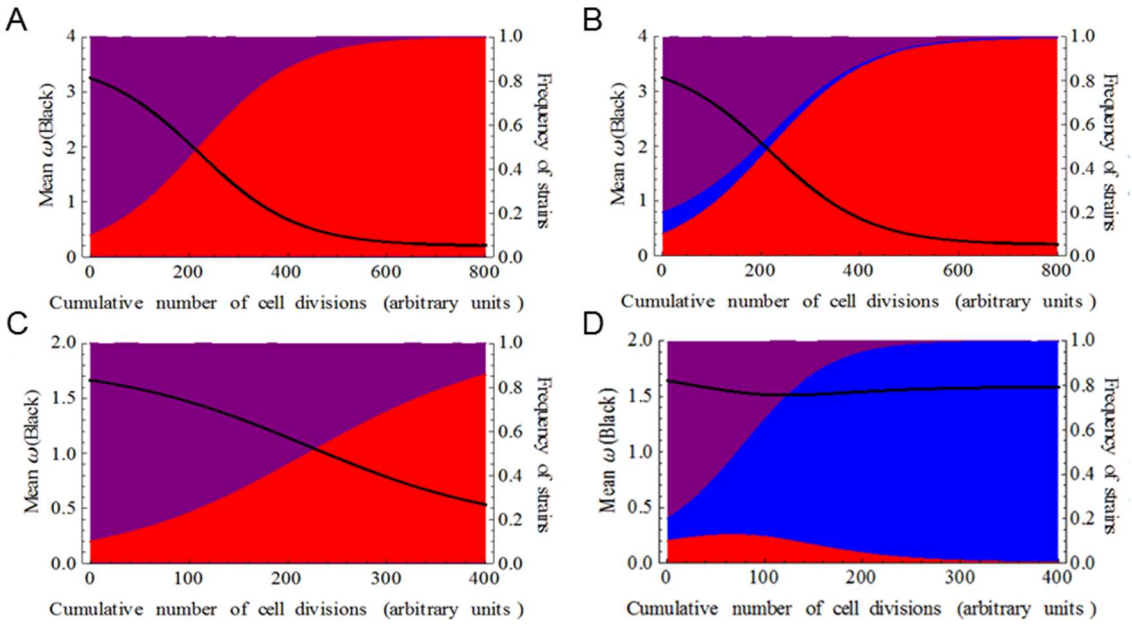


**Fig. S14.** Four scenarios in Fig. 3 *A* – *D* simulated using the mathematical model for the 3-way public good game without QS regulation. Left Y-axes show $\bar{\omega}$, the mean fitness of the entire population, which is a proxy of $OD_{600}$ or CFUs/ml values prior to subculture (black lines). Right Y-axes show the frequencies of $p_{coop}$ (e.g. WT, purple), $p_{ch1}$ (e.g. *lasR*, red) and $p_{ch2}$ (e.g. *pvdS,* blue). X-axes show the cumulative number of cell divisions as arbitrary units. The values that are given to the parameters of the simulations are: **(*A*)** $p_{coop}(0)=0.9$, $p_{ch1}(0)=0.1$, $p_{ch2}(0)=0$, $c_1=0.01$, $b_1=3.4$, $c_2=0$, $b_2=0$, $\omega_0=0.2$; **(*B*)** $p_{coop}(0)=0.8$, $p_{ch1}(0)=0.1$, $p_{ch2}(0)=0.1$, $c_1=0.01$, $b_1=3.4$, $c_2=0$, $b_2=0$, $\omega_0=0.2$; **(*C*)** $p_{coop}(0)=0.9$, $p_{ch1}(0)=0.1$, $p_{ch2}(0)=0$, $c_1=0.01$, $b_1=1.5$, $c_2=0.025$, $b_2=0.25$, $\omega_0=0.1$; **(*D*)** $p_{coop}(0)=0.8$, $p_{ch1}(0)=0.1$, $p_{ch2}(0)=0.1$, $c_1=0.01$, $b_1=1.5$, $c_2=0.025$, $b_2=0.25$, $\omega_0=0.1$. Note that the values of parameters used in these simulations are chosen to reflect approximately the relation between the values observed in Fig. 1, Fig. S1, Fig. 2, and Fig. 3.

**Supplementary text supporting Fig. S15:**

**pvdS *mutant can reach fixation.*** Our mathematical model predicts that mutants which are winning in a competition (*lasR* or *pvdS*) would reach fixation in our propagation experiments. We experimentally tested whether this would happen if the propagation were prolonged in competitions with initial mutant frequencies similar to those at the 18$^{th}$ day of the competitions in Fig. 3*D*. The results in Fig. S15 below show that when the competitions are initiated with *pvdS* frequencies similar to those at day 18 in Fig. 3*D*, *pvdS* always reaches to fixation when co-cultured either with WT (Fig. S15 *A*, *B*, and *C*), or with WT and *lasR* mutant (Fig. S15 *D*, *E*, and *F*).

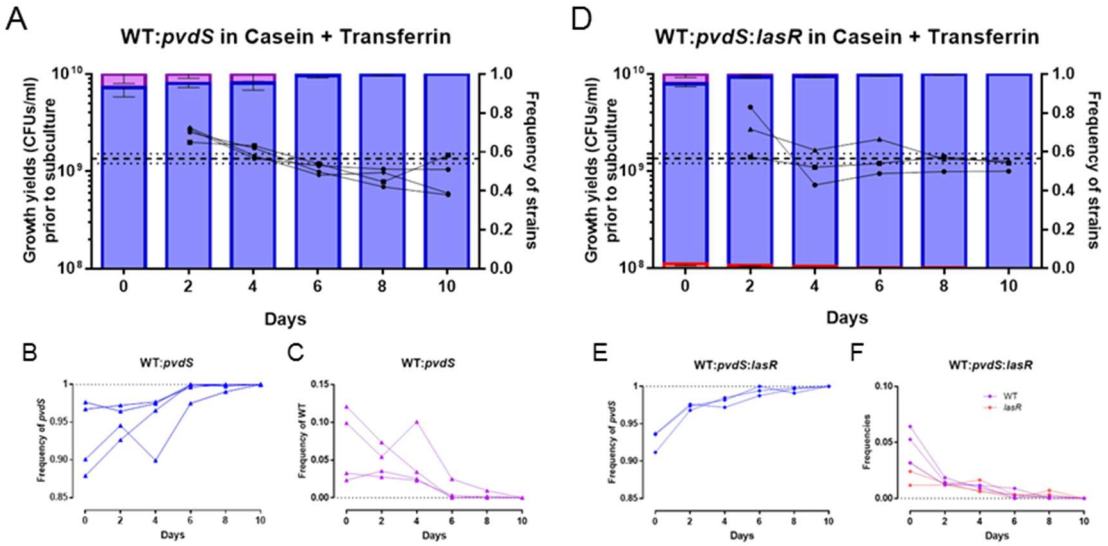


**Fig. S15.** Propagations of WT:*pvdS* (**(*A*)**, **(*B*)**, and **(*C*)**) and WT:*lasR*:*pvdS* cultures (**(*D*)**, **(*E*)** and **(*F*)**) in iron-depleted casein media throughout 10 days by passing the cultures to fresh media with a 1/1000 dilution after each 48 hours of growth ('X' axes show the days of propagation and the initial frequencies are shown at day 0). **(*A*)** Frequency changes of WT (purple) and *pvdS* (blue) in WT:*pvdS* co-cultures shown as stacked bars (right 'Y' axes) as the growth yields (CFUs/ml) of 4 biological replicates are shown as black lines (left 'Y' axes). **(*B*)** A detailed presentation of the frequency changes of *pvdS* in WT:*pvdS* co-cultures (blue). **(*C*)** A detailed presentation of the frequency changes of WT in WT:*pvdS* co-cultures (purple). **(*D*)** Frequency changes of WT (purple), *pvdS* (blue), and *lasR* (red) in WT:*pvdS*:*lasR* co-cultures shown as stacked bars (right 'Y' axes) as the growth yields (CFUs/ml) of 3 biological replicates are shown as black lines (left 'Y' axes). **(*E*)** A detailed presentation of the frequency changes of *pvdS* in WT:*pvdS* co-cultures (blue). **(*F*)** A detailed presentation of the frequency

changes of WT (purple), and *lasR* (red), in WT:*pvdS*:*lasR* co-cultures. Dash lines indicate the mean monoculture *pvdS* growth yields in the same media and the dotted lines indicate SD in (*A*) and (*D*) (mean:$1.35x10^9$ CFUs/ml; ±SD=$1.12x10^0$ CFUs/ml). Dotted lines indicate full fixation of *pvdS* to 100% of the population in (*B*), (*C*), (*E*) and (*F*). For (*A*), (*B*), and (*C*) N=4; and for (*D*), (*E*), and (*F*) N=3.

**Supplementary text supporting Fig. S16 – 19:**

**Simulations of other possible scenarios.** We also simulated alternative scenarios in an environment where both traits are needed **without QS regulation** or **with QS regulation** (only the 1st cooperative trait is regulated by QS):

**(A)** When only the cooperator of both cooperative traits (e.g. WT) and the cheater of the 2nd cooperative trait (which is not regulated by quorum sensing, e.g. *pvdS*) are in competition, the cheater wins and reaches to fixation as in the triple co-culture scenario, regardless of QS regulation of the 1st cooperative trait **(Fig. S16)**, while the mean fitness becomes: $\bar{\omega} = \omega_0 + b_1 - c_1$;

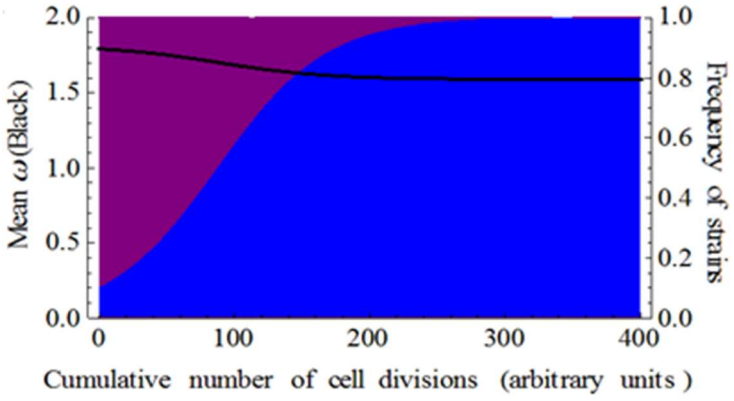


**Fig. S16.** Simulation with two strains, full cooperator (WT) + cheater for the 2nd cooperative trait, under conditions where both public goods are produced and $c_2 > c_1$. Left Y-axis show $\bar{\omega}$, the mean fitness of the entire population which is a proxy of $OD_{600}$ or CFUs/ml values prior to subculture (black lines). Right Y-axis show the frequencies of $p_{coop}$ (purple), and $p_{ch2}$ (blue). X-axis shows the cumulative number of cell divisions as arbitrary units. The values given to the parameters of the simulations were: $p_{coop}(0)=0.9$, $p_{ch1}(0)=0$, $p_{ch2}(0)=0.1$, $c_1=0.01$, $b_1=1.5$, $c_2=0.025$, $b_2=0.25$, $\omega_0=0.1$. The results were the same regardless if the 1st was considered to be regulated by QS (n=30, th=0.8) or not (n=0, th=0).

**(B)** When only **two cheaters are in 1:1 competition**, the cheater that saves the greater cost (here, the cheater of the 2nd cooperative trait since $c_2 > c_1$) wins the competition and reaches to fixation regardless of QS regulation of the 1st cooperative trait **(Fig. S17)**, while the mean fitness becomes: $\bar{\omega} = \omega_0 + b_1 - c_1$;

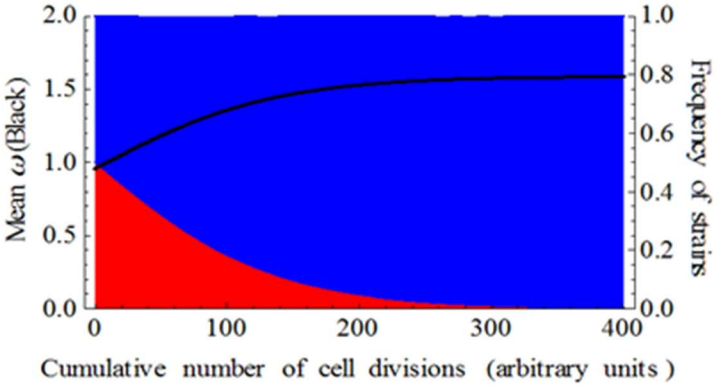


**Fig. S17.** Simulation with the two cheaters competing with each other, under conditions where both public goods are produced and $c_2>c_1$. Axes as in Fig. S16. Frequencies of $p_{coop}$ (purple), $p_{ch1}$ (red), and $p_{ch2}$ (blue) are shown. The values given to the parameters of the simulations were: $p_{coop}(0)=0$, $p_{ch1}(0)=0.5$, $p_{ch2}(0)=0.5$, $c_1=0.01$, $b_1=1.5$, $c_2=0.025$, $b_2=0.25$, $\omega_0=0.1$. The results were the same regardless if QS regulation for the 1st cooperative trait was considered (n=30, th=0.8) or not (n=0, th=0).

**(C)** When the cooperator of the both cooperative traits (e.g. WT) is competing with two mutants under conditions where the costs of both traits are equal (**$c_1=c_2$**), both cheaters increase in frequency until both of them reach 50% of the population **(Fig. S18)**, similarly with or without QS regulation of the 1st cooperative trait, while the mean fitness becomes: $\bar{\omega} = \omega_0 + ½ (b_1 + b_2 - c_1 - c_2)$**.**

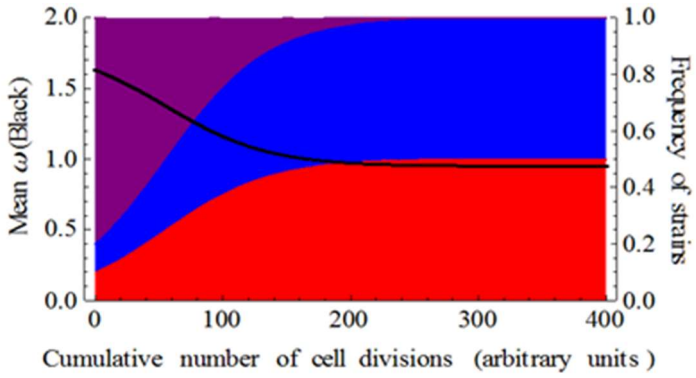


**Fig. S18.** Simulation for a 3-way competition with the cooperator of the both cooperative traits competing with two cheaters, under conditions where both public goods are produced and **$c_2=c_1$**. Axes as in Fig. S16. Frequencies of $p_{coop}$ (purple), $p_{ch1}$ (red), and $p_{ch2}$ (blue) are shown. The values given to the parameters

of the simulations were: $p_{coop}(0)=0.8$, $p_{ch1}(0)=0.1$, $p_{ch2}(0)=0.1$, $c_1=0.025$, $b_1=1.5$, $c_2=0.025$, $b_2=0.25$, $\omega_0=0.1$.The results were the same regardless if QS regulation for the 1st cooperative trait was considered **(**n=30, th=0.8) or not (n=0, th=0).

**(D)** When the cooperator of the both cooperative traits (e.g. WT) is competing with two mutants under conditions where the **$c_1>c_2$**, then the more drastic tragedy inducing cheater becomes the winner of the 3-way competition. In this case, when the 1st cooperative is not regulated by QS, the cheater of the 1st cooperative trait wins the 3-way competition and causes a drastic collapse, with the mean fitness: $\bar{\omega} = \omega_0 + b_2 - c_2$ **(Fig. S19*A*)**.

However, when the 1st cooperative trait is regulated by QS, the cheater of the 1st cooperative, while it still wins the competition, it can only increase in frequency until the QS threshold (th=0.8) and thus, cannot reach to fixatiob **(Fig. S19*B*)**; and the mean fitness becomes:

$$\omega_0 + (b_1 - c_1)\,(0.4) + (b_2 - c_2)\,(0.8)$$

As a result, the the cooperator of the both cooperative traits (e.g. WT) persists in the population. Therefore, presumably the population has a greater chance to recover, if the environmental conditions change. In conclusion, the QS regulation becomes relevant only under conditions where the mutant for the QS-regulated trait (here the cheater of the 1st cooperative trait) is not completely outcompeted.

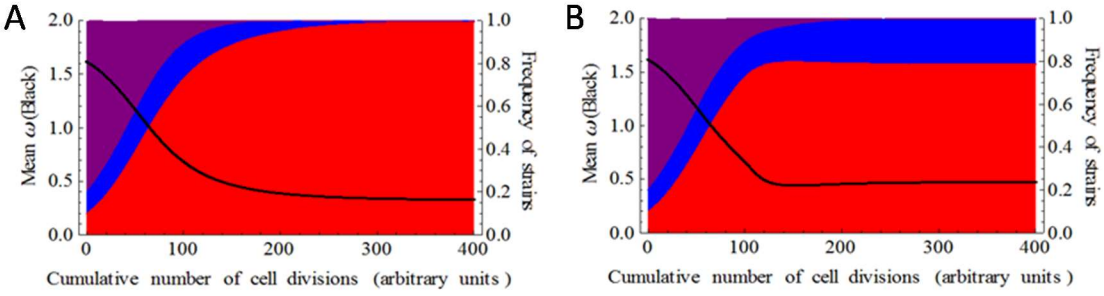


**Fig. S19.** Simulation for a 3-way competition with the cooperator of the both cooperative traits competing with two cheaters, under conditions where both public goods are produced and **$c_1>c_2$**. Axes as in Fig. S16. Frequencies of $p_{coop}$ (purple), $p_{ch1}$ (red) and $p_{ch2}$ (blue) are shown. The values given to the parameters of the simulations were: ***(A)*** $p_{coop}(0)=0.8$, $p_{ch1}(0)=0.1$, $p_{ch2}(0)=0.1$, $c_1=0.04$, $b_1=1.5$, $c_2=0.025$, $b_2=0.25$, $\omega_0=0.1$, n = 0, th = 0; ***(B)*** same as in (*A*) except n=30 and th=0.8, as QS regulation was considered for the 1st cooperative trait.